STATE OF ALASKA

DEPARTMENT OF NATURAL RESOURCES

DIVISION OF GEOLOGICAL AND GEOPHYSICAL SURVEYS

Walter J. Hickel, *Governor*

Harold C. Heinze, *Commissioner*

Thomas E. Smith, *Director and State Geologist*

November 1991

This report is a preliminary publication of DGGS. The author is solely responsible for its content and will appreciate candid comments on the accuracy of the data as well as suggestions to improve the report.

Report of Investigations 90-3

THE IGNEOUS PETROLOGY AND GEOCHEMISTRY OF NORTHERN AKUTAN ISLAND, ALASKA

By
J.D. Romick

STATE OF ALASKA
Department of Natural Resources
DIVISION OF GEOLOGICAL & GEOPHYSICAL SURVEYS

According to Alaska Statute 41, the Alaska Division of Geological and Geophysical Surveys is charged with conducting "geological and geophysical surveys to determine the potential of Alaskan land for production of metals, minerals, fuels, and geothermal resources; the locations and supplies of ground water and construction materials; the potential geologic hazards to buildings, roads, bridges, and other installations and structures; and shall conduct such other surveys and investigations as will advance knowledge of the geology of Alaska."

In addition, the Division of Geological and Geophysical Surveys shall collect, record, evaluate, and distribute data on the quantity, quality, and location of underground, surface, and coastal water of the state; publish or have published data on the water of the state and require that the results and findings of surveys of water quality, quantity, and location be filed; require that water-well contractors file basic water and aquifer data, including but not limited to well location, estimated elevation, well-driller's logs, pumping tests, flow measurements, and water-quality determinations; accept and spend funds for the purposes of AS 41.08.017 and 41.08.035, and enter into agreements with individuals, public or private agencies, communities, private industry, and state and federal agencies; collect, record, evaluate, archive, and distribute data on seismic events and engineering geology of the state; and identify and inform public officials and industry about potential seismic hazards that might affect development in the state.

Administrative functions are performed under the direction of the State Geologist, who maintains his office in Fairbanks. The locations of DGGS offices are listed below:

· 794 University Avenue
(Suite 200)
Fairbanks, Alaska 99709-3645
(907) 474-7147

· 400 Willoughby Avenue
(3rd floor)
Juneau, Alaska 99801
(907) 465-2533

· 18225 Fish Hatchery Road
P.O. Box 772116
Eagle River, Alaska 99577
(907) 696-0070

This report, printed in Fairbanks, Alaska, is for sale by DGGS for $3. DGGS publications may be inspected at the following locations. Address mail order to the Fairbanks office.

· 794 University Avenue
(Suite 200)
Fairbanks, Alaska 99709-3645

· 400 Willoughby Avenue
(3rd floor)
Juneau, Alaska 99801

· U.S. Geological Survey
Earth Science Information Center
605 West 4th Avenue, Room G684
Anchorage, Alaska 99501

· U.S. Geological Survey
Earth Science Information Center
4230 University Drive, Room 101
Anchorage, Alaska 99508

CONTENTS

CONTENTS (continued)

FIGURES

CONTENTS (continued)

TABLES

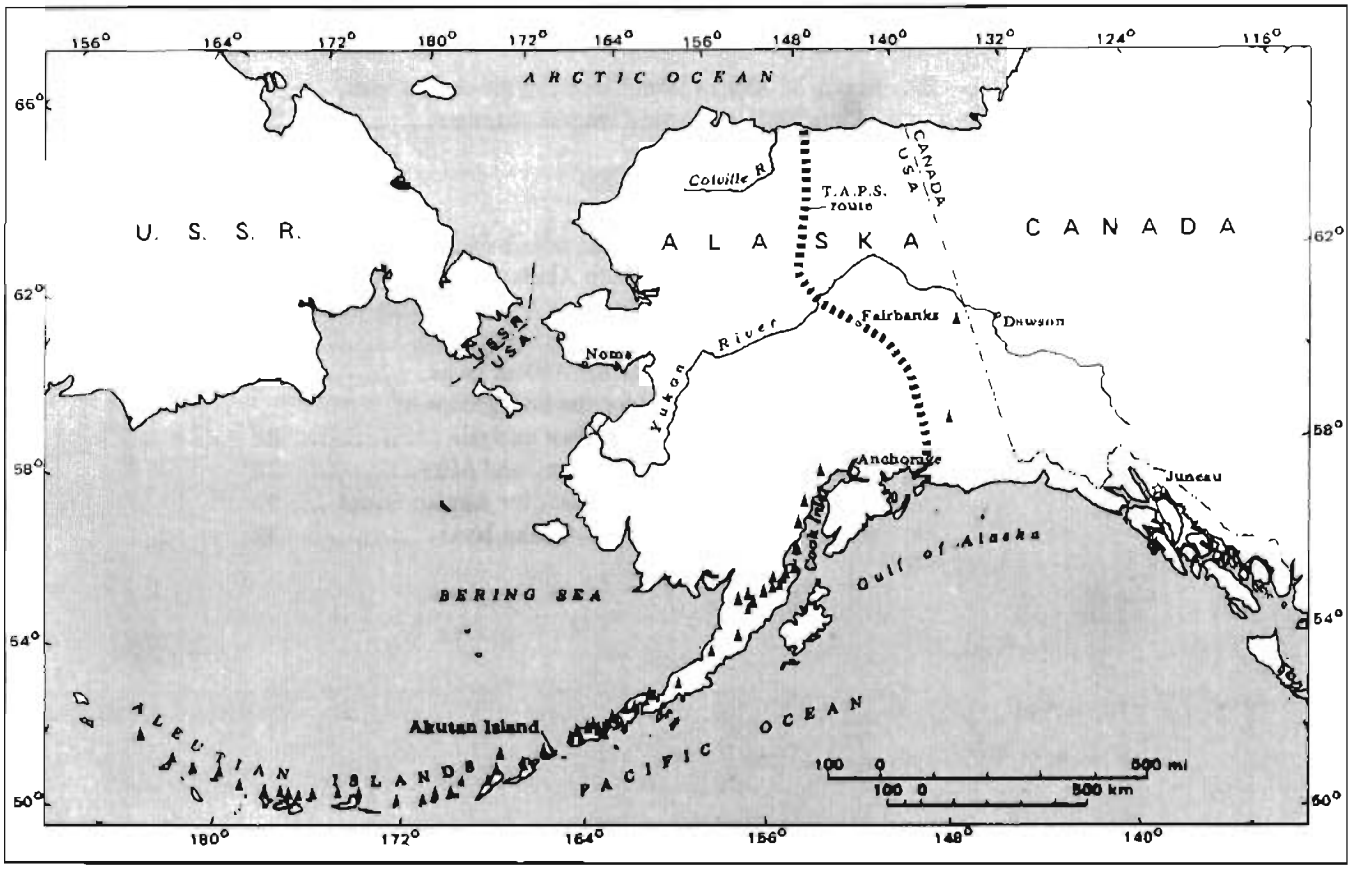

Figure 1. *Position of Akutan Island within the Aleutian Arc. Triangles represent volcano locations along the arc.*

THE IGNEOUS PETROLOGY AND GEOCHEMISTRY OF NORTHERN AKUTAN ISLAND, ALASKA

By
J.D. Romick[1]

ABSTRACT

Volcanism on Akutan Island, in the eastern Aleutian Arc, is characterized by tholeiitic lavas ranging between 46 and 63 weight-percent SiO_2, with FeO*/MgO ratios between 1.3 and 4.2. Olivine-augite-plagioclase basalts were found at Lava Peak; the other flows and dikes on the island consist of hypersthene-augite-plagioclase basalts and andesites. The Lava Peak basalts had < 23 ppm Rb and > 400 ppm Sr, whereas the other lavas sampled had higher concentrations of Rb and lower concentrations of Sr. K-Ar whole-rock dates of lava flows and dikes indicate that they erupted between 1.5 and 1.1 Ma ago. Clinopyroxene, orthopyroxene, and olivine compositions are uniform across the island, and average $Ca_{43}Mg_{42}Fe_{17}Si_2O_6$, $Mg_{66}Fe_{34}SiO_3$, and $Mg_{72}Fe_{28}Si_2O_4$, respectively. Plagioclase compositions vary between An_{93} and An_{51} with the more calcic plagioclase being restricted to the Lava Peak basalts. The chemical trends seen in Akutan lavas are consistent with the shallow-level fractionation of olivine, plagioclase, and clinopyroxene from a parental liquid and subsequent eruption of magmas from different levels of a zoned magma chamber.

ACKNOWLEDGMENTS

I thank the Geothermal program of the Alaska Division of Geological and Geophysical Surveys (DGGS) for funding this study. Roman Motyka (DGGS) conducted the microprobe analyses on samples collected, and without his generous support this thesis would not have been possible. I also thank M.W. Wiltse for analyzing my samples. Michael Perfit was very gracious in allowing me to use some of his unpublished data on Akutan lavas. My thanks go to my committee for their helpful comments and criticisms on various drafts (which greatly improved the text), to my fellow graduate students for their comments on my ideas, and to my wife, Jan, whose drafting skill and patience made this thesis a great deal easier. Additional reviews by Robert Kay, Michael Perfit, and Chris Nye greatly improved the text of this report.

Finally, I take credit for whatever insights the reader may glean from this study and the blame for any errors that appear.

INTRODUCTION

The purpose of this study is to characterize the mineralogy, petrology, and geochemistry of the volcanic rocks exposed on northern Akutan Island.

GEOGRAPHIC SETTING

Akutan Island is located in the eastern Aleutian chain at 54°05' N. and 165°55' W., about 45 km northeast of Unalaska Island (fig. 1). Commercial access to Akutan Island is limited to air service (by Grumman Goose) and boat charter out of Dutch Harbor on Unalaska Island to Akutan Village. Akutan Village is located on the east side of the island in Akutan Harbor (fig. 2). The village was established in 1879 as a fur trading post, and subsequently operated as a whale-processing station. The present population of approximately 120 people depend upon commercial and subsistence fishing, and hunting, for their livelihood. Several fish processors operate out of Akutan Harbor during the summer months (Morgan, 1980, Motyka and others, 1988).

The island is 29 km long, 21 km wide, and oriented roughly east-west (fig. 2). It is dominated by Akutan Volcano, an active 1,304-m-high composite volcano. Central and eastern Akutan Island consist of steep ridges separating glacially scoured valleys that radiate away from the volcano. Western Akutan has a gentle topography dissected by streams flowing off the west flanks of the volcano.

[1]Dow Chemical U.S.A., 1602 Building, Midland, Michigan 48640

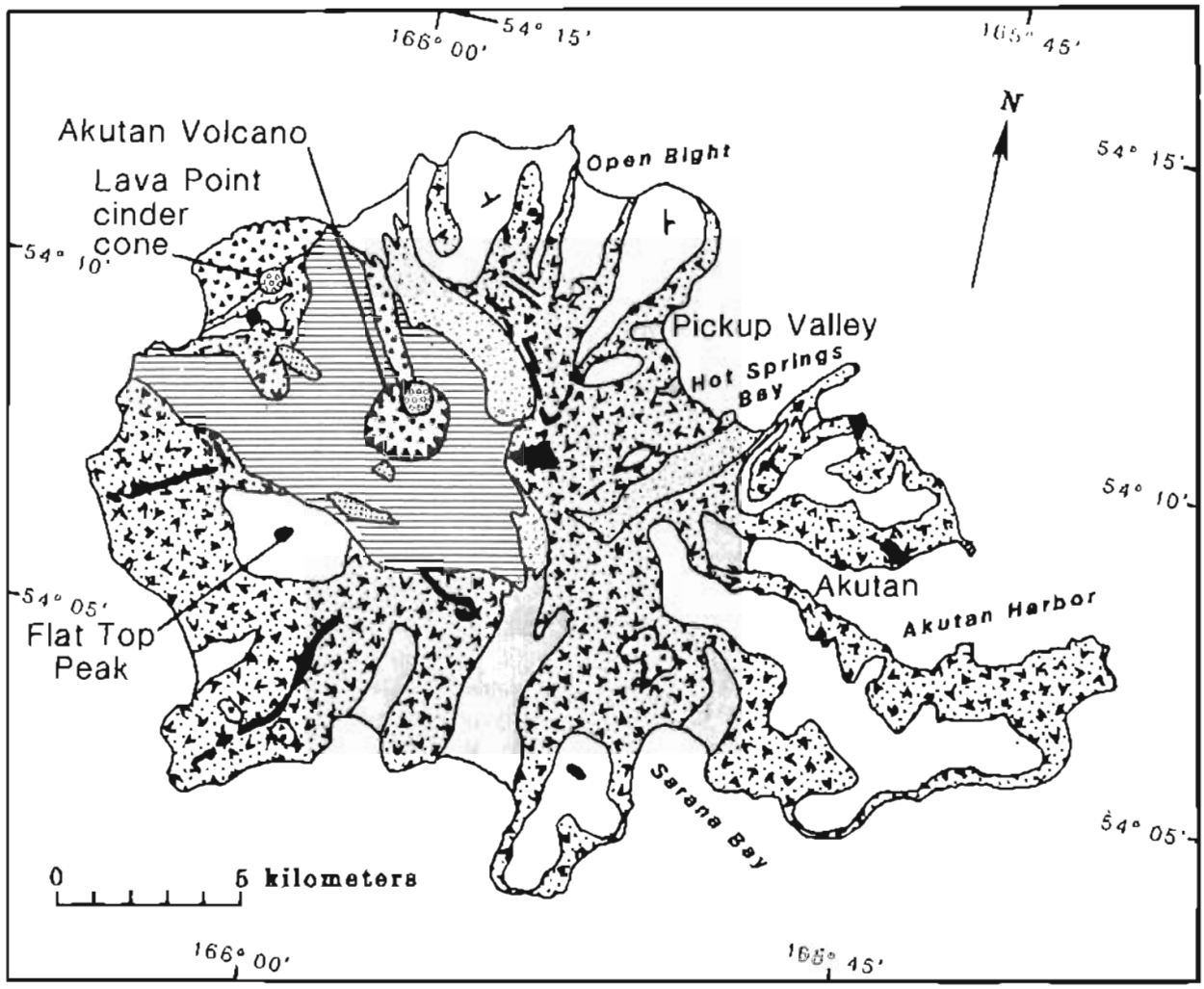

EXPLANATION

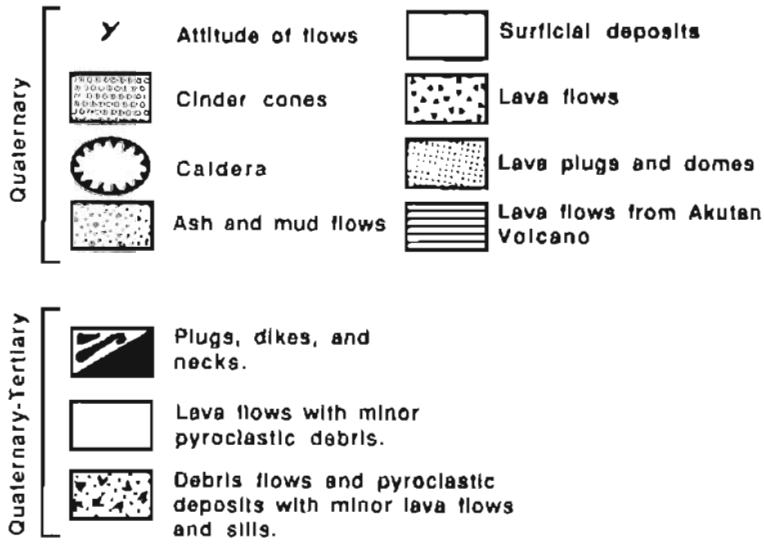

Figure 2. *Generalized geologic map of Akutan Island. Adapted from Byers and Barth (unpublished); Swanson and Romick, 1988.*

The summit of Akutan Volcano contains a 2-km-wide caldera, which may have been formed within the last 500 yr (Byers and Barth, 1953). Within the caldera is a cinder cone, which existed prior to 1931 (Finch, 1935), and a small lake. The caldera is breached on the north side. Northwest of the volcano are two small eruptive centers: an old eroded volcanic center consisting primarily of lava flows, and a cinder cone with two lava flows that erupted sometime before 1870 (Byers and Barth, 1953).

PREVIOUS WORK

R.H. Finch conducted the first scientific exploration of the island in 1931. He was a member of the U.S. Geological Survey's (USGS) Volcanology section conducting studies of the Aleutian volcanoes in preparation for the establishment of a volcano observation post. Akutan Island was examined because its frequent eruptive activity and relative accessibility made it a convenient place for observation. The result of Finch's (1935) study was a brief description of the geology and a topographic sketch of the island. Finch noted that Dr. T.A. Jaggar had visited the island in 1907 and 1927 and had made some correlations between the sedimentary units on Akutan and those on the Alaska Peninsula, but nothing was published regarding that correlation.

Byers and Barth (USGS) conducted field work on Akutan Island in 1948 as part of the USGS study of the Aleutian Islands after World War II, but no official report was issued. Their geologic map of Akutan Island (unpublished) was obtained from the USGS archives, in Menlo Park, by Motyka (DGGS). Byers and Barth (1953) discussed the 1947 and 1948 eruptions on Akutan Island, but not past volcanic activity or geology of the island.

Perfit and Kay did some reconnaissance mapping and sampling of the island in 1974 and the initial results were presented by Perfit (1978). Motyka and others (1981) provided a brief description of Akutan geology, but emphasized the geothermal resources of the island. Perfit and Gust (1981) published some isotope and microprobe analyses of samples from Akutan Island and discussed how their results related to those of other Aleutian Islands. McCulloch and Perfit (1981) published isotope and rare-earth-element data for Akutan lavas and used the data to develop constraints for magma genesis in the Aleutian Islands.

GENERAL GEOLOGY

Figure 2 is a copy of the general geology of Akutan Island adapted from Byers and Barth (unpublished map) and slightly modified by Swanson and Romick (1988). Akutan Island consists of interbedded lava flows and volcaniclastic deposits overlain in places by younger volcanic deposits as sociated with Akutan Volcano. The interbedded flows and volcaniclastic material represent older deposits principally exposed on central and eastern Akutan Island. Some of the older rocks are slightly to moderately altered and contain secondary chlorite and carbonate, whereas the younger volcanics are largely unaltered.

The older rocks can be divided into two units: a lower unit of at least 700 m of volcaniclastic deposits with interbedded flows and sills and an upper unit dominated by basaltic to andesitic flows with lesser amounts of interbedded volcaniclastic deposits (Motyka and others, 1981).

The older lavas are exposed in glacial valleys whose bottoms are filled with alluvium, stream sediments and, in at least one case, volcanic debris-flow deposits. Exposures along the coast indicate that sea level was considerably lower when the valleys were formed; valley walls can be traced below present sea level. Black (1974) indicated that deglaciation occurred 8,400 years ago for Umnak Island (160 km west of Akutan Island). Considering the proximity of Akutan Island to Umnak, it seems reasonable to assume that deglaciation occurred on Akutan at roughly the same time. Landsat images of Akutan show that the radial glacial valleys on the island were carved before formation of present Akutan Volcano.

Associated with the older rocks are numerous dikes, concentrated in Hot Springs Bay, which decrease in abundance eastward. Dikes located around Hot Springs Bay Valley strike northwest. Those located to the west of Hot Springs Bay Valley are generally oriented northeast, but dike orientations span 180°. Gabbroic intrusions are associated with the older volcanic complex. A large sill in Sandy Cove is exposed over 150 m, whereas a smaller intrusion is exposed in the cliff on the west side of Hot Springs Bay. The orientation and arrangement of several linear intrusions, exposed south of Open Bight (fig. 2), suggests that they may be ring dikes associated with an older caldera system. Dip measurements on the map prepared by Byers and Barth (unpublished) also suggest an older center of volcanic activity near Open Bight (fig. 2).

On northwestern Akutan Island is a 594-m-high ridge, here called Lava Peak, where at least 19 flows and seven dikes are exposed. The flows are separated into two groups by an unconformity (fig. 3). Eleven almost flat-lying flows are overlain by at least eight flows with a 24° apparent dip to the west.

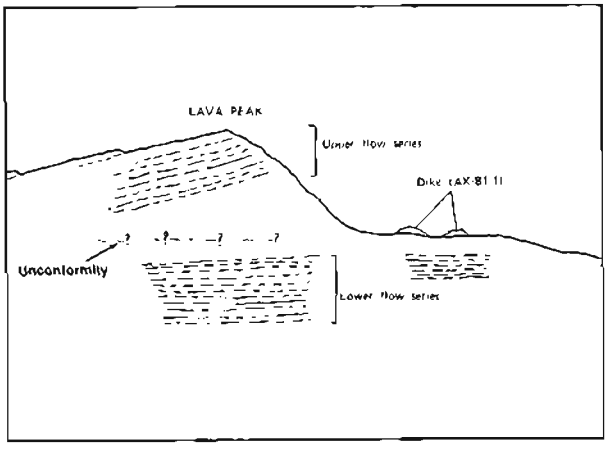

Figure 3. *Sketch of Lava Peak showing the relationship between the upper and lower flow series.*

Samples were collected from a section about 690 m thick. East of the peak is a highly baked, oxidized, autobrecciated zone characteristic of volcanic vents; it is probably the core of an eroded volcanic center.

The dikes that intrude these rocks are only exposed on the north side of the ridge and strike in a northwesterly direction. A large dike, exposed east of the flows, intrudes the lower 11 lava flows but is truncated by the upper sequence of flows. It is the backbone of the ridge to the east of the flows and may have been a feeder dike from Akutan Volcano during an older period of volcanism.

South of Lava Peak are several flows that are stratigraphically lower than the Lava Peak rocks and mantled by recent tephra deposits from Akutan Volcano.

North of Lava Peak is a cinder cone and two lava flows that probably formed before 1870 (Byers and Barth, 1953). Byers and Barth noted that the Russians made no mention of the cone or associated flows during their visit to the island in the 1870s and suggested that the eruptive activity occur before their visit. Simkin and others (1981) list an eruption on the northwest flank of the volcano in 1855, which may mark the eruption of the Lava Point cone and flows. The cone is about 250 m high and 600 m across. The flow occupies 4 km^2 and forms Lava Point (fig. 2).

Recent deposits include flows from 1947 and 1948 eruptions, which did not leave the summit, and the 1978 lava flow, which almost reached the north coast. The lava flow followed two stream drainages down the north flank of the volcano and came to within 1 km of the coast. Ash eruptions interspersed with these flows mantle some of the deposits on western Akutan Island, and reached Akutan Village, on the east side of the island (Finch, 1935; Byers and Barth, 1953). Table 1 shows volcanic activity on Akutan Island since 1790.

PETROLOGY

DISTRIBUTION

Igneous rocks on Akutan Island consist of older rocks exposed at Lava Peak and on the central and eastern part of the island, and younger rocks associated with Akutan Volcano, exposed on the western side of the island. Petrographic descriptions of Akutan lavas are cataloged in appendix A.

Table 1. *Volcanic activity on Akutan Island since 1790*

Date	Type of eruption	Location
1790	Smoking	
1828	Smoking	
1838	Smoking	
1845	Smoking	
March 1848	Small explosive eruption	
1852	Parasitic cone eruption	NW of Summit
1862	Smoking	
1865	Glow seen from Unimak Pass	
1867	?	
1883	Small steam and ash eruption	
1887	Lava flow	
1892	?	
1896	Glowing	
1907	Continuously active	
Feb. 22, 1908	Lava flow	
1911	Ash fell on Akutan Village	
1912	Smoking	
1928	Smoke and "flaming"	
May 1929	Explosive eruption and lava flow	
1931	Explosive eruption	
1946-47	Lava flow and explosive eruption	
1948	Explosive eruption	
Oct. 1951	Explosive eruption	
1953	?	
1972	Explosive eruption	
1974	Parasitic cone, ash eruption, and lava flow	West flank?
1976-77	Explosive eruptions	
Sept. 25, 1978	Lava flow and ash eruption	
1980	Explosive eruption	

Sources: Finch (1935), Byers and Barth (1953), and Simkin and others (1981).

WESTERN AKUTAN ISLAND

LAVA PEAK FLOWS

The lower section consists of 11 flows ranging from 1.7 to 12 m thick. The basal flow is the thickest flow exposed. Going upsection the flows thin and then thicken again. Several flows have baked brecciated upper zones, which grade downward into vesicular rock. All 11 flows contain plagioclase, olivine, and clinopyroxene phenocrysts in a fine-grained holocrystalline groundmass consisting of plagioclase, titanomagnetite, augite, and occasionally olivine (table 2). The rocks are fresh and generally unaltered, although some olivine has oxidized rims.

Figure 4 shows the mineralogic changes that occur going upsection, particularly olivine and clinopyroxene, which decrease markedly. The ratio of mafic phenocrysts to total phenocrysts decreases going up the section. There is a general decrease in the number of very large (3 to 7 mm) clinopyroxene phenocrysts upsection, as well as a decrease in the overall grain size of the clinopyroxene. Olivine phenocrysts remain about the same size and skeletal olivine crystals are present in all 11 flows. The abundance and size of plagioclase phenocrysts (except for the top flow) remain constant. In addition to the decrease of both olivine and clinopyroxene, there is a sympathetic relationship between the relative abundances of the two minerals. Figure 4 shows that when olivine abundance is at a maximum, clinopyroxene is at a minimum, and vice versa. There are no soil horizons or weathering zones separating one flow from another, indicating that they erupted over a fairly short time.

Table 2. *Modal analyses for western Akutan lavas*

Location	Sample	Plag	Ol	Cpx	Opx	Opq	GM
Lava Peak(D)	AK-81-1	18.4	4.2	11.4	–	1.0	65.0
Lava Peak(U)	AK-81-2	41.8	8.6	3.4	–	0.2	46.0
Lava Peak(U)	AK-81-3	36.8	3.2	8.0	–	0.4	51.2
Lava Peak(U)	AK-81-4	39.2	1.6	4.2	–	1.6	53.4
Lava Peak(L)	AK-81-5	41.0	2.4	7.6	–	1.0	48.0
Lava Peak(L)	AK-81-6	25.6	2.4	6.8	–	1.4	63.0
Lava Peak(L)	AK-81-7	24.4	4.4	6.6	–	1.0	63.0
Lava Peak(L)	AK-81-8	24.2	4.0	7.2	–	1.0	64.4
Lava Peak(L)	AK-81-9	27.2	5.4	4.8	–	2.0	60.6
Lava Peak(L)	AK-81-10	23.0	5.2	6.0	–	1.2	64.6
Lava Peak(L)	AK-81-11	20.4	7.0	6.8	–	1.2	64.6
Lava Peak(L)	AK-81-12	21.8	5.6	9.6	–	1.2	61.8
Lava Peak(L)	AK-81-13	18.4	5.2	4.6	–	2.0	69.4
Lava Peak(L)	AK-81-14	23.0	5.0	11.2	–	1.6	59.0
Lava Peak(L)	AK-81-15	15.4	4.8	6.8	–	2.0	70.0
Old flow	AK-81-16	17.0	1.0	3.0	–	0.75	79.0
Old flow	AK-81-17	14.0	0.75	8.0	3.0	1.0	74.0
Old flow	AK-81-18	35.0	1.8	7.6	0.4	2.0	53.2
Old flow	AK-81-31	30.0	tr.	–	–	–	70.0
1978 flow	AK-81-27	32.2	tr.	5.0	0.8	0.4	61.6
Pre-1870 flow	AK-81-35	26.0	0.2	1.2	–	0.2	72.4

D - dike, U - upper series, L - lower series, Plag - plagioclase, Ol - olivine, Cpx - clinopyroxene, Opx = orthopyroxene, Opq = opaques, GM - groundmass.

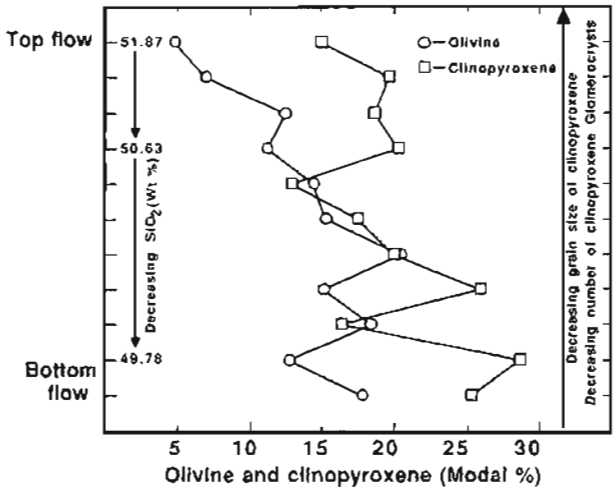

Figure 4. *Plot showing change in percentage of olivine and clinopyroxene in the lower flow series exposed on Lava Peak. Percentages were recalculated with olivine, clinopyroxene, and plagioclase phenocrysts only.*

Three flows were sampled from the upper part of the section. The exposure is very irregular, making it impossible to measure the thickness of the flows sampled. Individual thicknesses are estimated at between 2 and 5 m. The mineralogy of the three flows is identical to that of the lower flows. The rocks are porphyritic, with large clinopyroxene, plagioclase, olivine, and opaque minerals in a fine-grained holocrystalline groundmass. The percentage of olivine in the three flows is highly variable and ranges between 8.6 for the top flow and 1.6 for the bottom one. The olivine in all three flows has partially oxidized rims.

ASSOCIATED DIKES

Of the seven dikes intruding Lava Peak, the largest is exposed to the east of Lava Peak and is 10 to 15 m wide (AK-81-1; fig. 3, app. A). In thin section, the dike contains the same mineral assemblage as the Lava Peak flows; randomly oriented phenocrysts of olivine, clinopyroxene, opaque minerals, and plagioclase in a groundmass of opaque minerals, clinopyroxene, and plagioclase laths. A 1.5-m-wide zone of red rock near the dike may represent the baked contact between the dike and the country rock. The dike is truncated by the upper sequence of lava flows.

The six other dikes sampled stand out as resistant spines on the north side of Lava Peak. The dikes range in thickness from 0.5 to 4 m and are oriented N. 70° W. Except for the westernmost dike, the dikes are aphanitic in hand specimen. They contain bands of vesicles aligned parallel to the walls of the dike with individual vesicles elongate in the same direction. This is probably due to cooling from the outside inward, forcing exsolving volatiles toward the center of the dike. Movement of the cooling magma stretched the vesicles in the direction of flow.

The dikes intrude a series of interbedded lava and debris flows located at 100 m elevation. The baked contact of these dikes is 1 to 2 cm thick. Columnar jointing is moderately well developed and is oriented perpendicular to the walls of the dike.

In thin section, the dikes vary from equigranular fine grained to porphyritic. Plagioclase is the dominant phenocryst. In several dikes olivine and clinopyroxene are as abundant as plagioclase. The smaller dikes (AK-81-32, -33, -34, -103A, and -103B) show a strong alignment of plagioclase laths in the groundmass. Several of the dikes contain interstitial brown glass.

OTHER FLOWS

These flows are located stratigraphically below the Lava Peak flows and are similar to lavas exposed on the central and eastern side of the island.

The three flows sampled were interbedded with debris flows consisting of a clay-rich matrix with blocks ranging up to several meters high. Sample AK-81-16 is from a 7-m-thick flow exposed in a canyon wall. It has a scoriaceous top and flow banding. The lava contains about 17 percent plagioclase phenocrysts and very little clinopyroxene and olivine. The groundmass is very fine grained and makes up about 80 percent of the rock. The two other flows sandwich AK-81-16 and contain plagioclase along with varying amounts of hypersthene and clinopyroxene, with trace amounts of olivine and opaque minerals. The groundmass in these rocks is very fine grained and makes up to 75 percent of the rock.

RECENT LAVAS

The most recent volcanism on Akutan Island resulted in tephra deposits, the eruption of two lava flows, and a cinder cone on the north and northwest flank of Akutan Volcano. Sometime before 1870 a cinder cone developed just northeast of Lava Peak (fig. 2). A lava flow erupted from the base of the cone, covering about 4 sq km, and makes up what is called Lava Point (Byers and Barth, 1953). The lava flow is very blocky and has two lobes that enter the sea. Erosion has exposed numerous lava tubes on the northern border of the flow that have developed into spectacular bridges and caves. The rock is very vesicular and contains plagioclase phenocrysts with minor clinopyroxene, olivine, and opaque minerals in a glassy groundmass. The groundmass contains oriented plagioclase laths, some opaque minerals, and a great deal of brown glass.

In 1978 a lava flow erupted in the summit caldera, flowed down the north flank of Akutan Volcano in two lobes, and came within 1 km of the coast (fig. 2). The flow consists of very blocky lava ranging from vesicular to glassy.

Plagioclase makes up about 32 percent of the rock; clinopyroxene, olivine, and opaque minerals make up less than 7 percent. The groundmass consists of oriented plagioclase laths and brown glass.

CENTRAL AND EASTERN AKUTAN ISLAND

OPEN BIGHT

Open Bight is the next valley east of the 1978 lava flow. Samples were collected from two flows(?) exposed at the mouth of the valley. Contacts were concealed so it is unclear whether the rocks are flows or sills. About 31 m of the upper flow(?) is exposed. Its lower section has large columnar joints; the upper section is massive. The other sample was collected from a 2- to 5-m-thick flow(?) exposed farther down the cliff. Both rocks contain about 32 percent plagioclase, 5 to 8 percent clinopyroxene, trace amounts of orthopyroxene, and 1 to 2 percent opaque minerals in a trachytic groundmass. Crystal clots of plagioclase, clinopyroxene, and opaque minerals are present. Plagioclase phenocrysts commonly contain glass inclusions.

HOT SPRINGS BAY VALLEY FLOWS

Three valleys empty into Hot Springs Bay, the largest being Hot Springs Bay Valley. Samples were collected along the coast and within the valleys. The small central valley was not explored. The westernmost valley is here called Pickup Valley (fig. 2).

PICKUP VALLEY

Samples were collected from the head and walls of Pickup Valley (table 3, fig. 2). Two samples, AK-81-20 and -21, were collected from outcrops described by Byers and Barth (unpublished map, 1948) as possible ring dikes. The samples are porphrytic and contain randomly oriented plagioclase, clinopyroxene, and opaque phenocrysts in a trachytic groundmass. The groundmass is slightly altered to chlorite and carbonate. Quartz-carbonate veinlets crosscut the groundmass and phenocrysts.

Table 3. *Modal analyses for eastern and central Akutan lavas*

Location	Sample	Plag	Ol	Cpx	Opx	Opq	Alt	GM
HSBV(D)	AK-81-37	1.8	–	–	tr.	–	10.2	88.0
HSBV(D)	AK-81-38	7.8	tr.	2.4	–	1.2	1.6	87.0
HSBV(D)	AK-81-39	–	–	tr.	–	tr.	12.0	88.0
HSBV(D)	AK-81-40	20.4	–	0.2	–	–	–	79.4
HSBV(D)	AK-81-44	10.0	–	–	–	–	8.0	82.0
HSBV(D)	AK-81-46	23.6	–	5.4	–	–	8.2	62.8
HSBV(D)	AK-81-47	17.4	–	–	–	–	9.4	72.8
Op.Bt(F)	AK-81-51	31.8	–	5.0	0.8	2.2	–	60.2
Op.Bt(F)	AK-81-52	32.6	–	7.2	0.6	1.4	1.8	56.2
HSBV(F)	AK-81-63	28.8	–	–	–	0.4	–	70.8
HSBV(F)	AK-RM-7a	10.6	–	1.2	0.6	1.4	–	86.2
HSBV(F)	AK-RM-8	12.8	–	1.6	0.6	1.6	–	83.4
PV(F)	AK-81-21	20.0	–	7.0	–	1.0	7.0	65.0
PV(F)	AK-81-22	6.4	–	0.6	0.6	–	–	91.8
PV(F)	AK-81-24	20.6	5.4	5.2	–	tr.	tr.	68.8
HSBV(I)	AK-81-102	19.6	0.4	3.4	–	–	–	76.6
PV(I)	AK-81-20	17.4	0.4	3.6	tr.	1.0	–	77.6

HSBV - Hot Springs Bay Valley, Op.Bt - Open Bight, PV - Pickup Valley,I - intrusion, F - lava flow, D - dike, Plag - plagioclase, Ol - olivine, Cpx - clinopyroxene, Opx - orthopyroxene, Opq - opaques, Alt - alternation minerals, GM - groundmass.

A lava flow exposed west of these samples has a baked lower contact and crudely developed columnar joints. The rock contains a few plagioclase phenocrysts in a very fine grained trachytic groundmass and is partially altered to chlorite, carbonate, and iron oxide.

Two samples were collected partway down the valley. AK-81-23 contains plagioclase, clinopyroxene, and orthopyroxene, whereas AK-81-24 contains partially altered olivine, plagioclase, and clinopyroxene. Both rocks contain chlorite and carbonate alteration in a holocrystalline trachytic groundmass.

COW POINT

Cow Point is a high bluff separating Pickup Valley from the unnamed valley to the southeast. Twenty-five dikes are exposed in this bluff and have a dominant trend to the northeast, but there is a very wide variability in strike. The dip for the dikes is quite variable and may range from 0° to 180° for a single dike. They also occur in nested groups of three or more.

Mineral banding is fairly common in these dikes. The banding consists of vertical layers with mafic minerals concentrated toward the interior and felsic minerals concentrated toward the exterior (fig. 5). This phenomenon has been studied by several workers (Bhattacharji and Smith, 1964; Gibb, 1972; Komar, 1972a,b). The mineral segregation seems to be the result of mechanical interactions between phenocrysts during intrusion, forcing early-forming minerals toward the center of the dike.

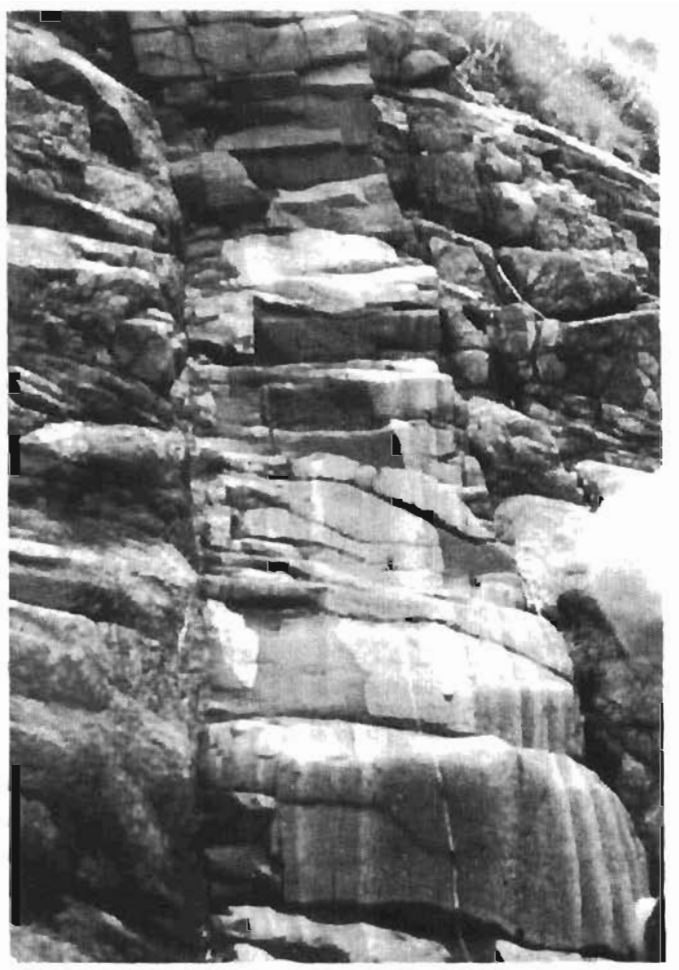

Figure 5. *Mineral banding in a Cow Point dike. The dike is about 1 m across.*

The dikes intrude pyroclastic deposits of poorly sorted volcanic breccia. Some dikes have fine-grained chilled margins where they contact the pyroclastic debris. Higher on the bluff are several oxidized layers that may represent the lava flows that baked the underlying debris flows.

In hand specimen, the dikes range from porphyritic-containing plagioclase phenocrysts to-aphanitic. Olivine and clinopyroxene are rare phenocrysts. This lack of mafic minerals is probably due to their alteration to the chlorite present in these rocks. Pseudomorphs of chlorite after clinopyroxene are occasionally seen. The most common groundmass consists of a trachytic mass of plagioclase laths and chlorite. Occasionally the groundmass is composed of an equigranular mixture of plagioclase, clinopyroxene, and opaque minerals.

FLOWS

Five flows, sampled from the northeast side of Hot Springs Bay Valley, range in thickness from 3.5 to 10 m where exposed. They contain plagioclase, clinopyroxene and, rarely, olivine phenocrysts. The groundmass ranges from fine to medium-grained holocrystalline in texture and shows no preferred orientation. Mafic minerals in the groundmass are partially altered to chlorite and carbonate. Sample AK-81-65 is the only flow sampled where olivine made up a significant proportion of the phenocrysts. Most of the rocks have some chlorite alteration, and in AK-81-65 the olivine is partially oxidized.

Five lava flows exposed farther upvalley differ from lower ones in that they are almost completely unaltered, except for rare carbonate grains. They are very fine grained rocks and consist of phenocrysts of plagioclase, clinopyroxene, orthopyroxene, and opaque minerals in a holocrystalline groundmass. Opaque minerals are unusually abundant, composing 1.4 to 1.6 percent of the rocks.

HOT SPRINGS BAY VALLEY DIKES

Nine variably altered dikes were sampled at the mouth of Hot Springs Bay Valley. The dikes sampled ranged in width from 1.5 to 3 m. The dominant orientation of these dikes is N. 42° W., but orientations varied as much as 40°.

The rocks are porphyritic, with plagioclase being the most abundant phenocryst. Hornblende is present as a phenocryst in AK-81-43. Sample AK-81-46 contains 29 percent phenocrysts, but the dikes usually contain less than 15 percent phenocrysts. The groundmass is fine-grained, trachytic, and composed of plagioclase laths and opaque minerals. Xenoliths, present in some samples, are similar in composition and texture to the host dikes, but are usually more altered than the enclosing rocks.

The dikes contain chlorite and carbonate as alteration products, replacing mafic phenocrysts, microphenocrysts, and glass.

DIKES

Hot Springs Bay Valley dikes are oriented roughly N. 68° W. with a variation in attitude of about 40°. The dikes range in width from 0.5 to 5 m and also occur as dike swarms to 13 m wide. They have well-developed baked contacts, ranging in thickness from 1 to 4 cm. Vesicles are concentrated toward the center of the dikes and are partially filled with carbonate.

Alteration is quite variable not only between dikes but within them. Five samples were taken across a dike. The country rock (AK-81-106-1.5) intruded by the dike was partially altered to chlorite and carbonate. Alteration in the dike increases toward the center until all of the mafic minerals and part of the groundmass are altered.

The dikes are generally very fine grained with trachytic textures. Crystal clots, when present, consist of plagioclase, clinopyroxene, and opaque minerals. Plagioclase is the only individual phenocryst. The groundmass is usually composed of plagioclase laths, opaque minerals, chlorite, and carbonate. One dike (from the east side of Hot Springs Bay Valley), AK-81-71, contains hornblende. It is coarse-grained, rock consisting of plagioclase, hornblende, and orthopyroxene. Carbonate is present as an interstitial filling, with chlorite partially replacing plagioclase.

AKUTAN HARBOR FLOWS

The outcrop between Hot Springs Bay Valley and Akutan Harbor consists of a thick sequence of volcaniclastic deposits, with very few flows or dikes.

Two dikes and a thick lava flow are exposed on the north side of Akutan Harbor (AK-81-26, -102A, -102B). The flow is about 8 m thick with a lower section consisting of well-developed columnar joints. It is a very fine-grained equigranular rock with rare plagioclase phenocrysts and a holocrystalline groundmass consisting of clinopyroxene, plagioclase, and titano-magnetite. The plagioclase laths have a strongly preferred orientation. Except for a small amount of chlorite in the groundmass, the rock is unaltered.

The two dikes that intrude the flow are different in mineralogy and texture. Dike AK-81-102A, 1.5 m wide, is flow banded and contains only plagioclase phenocrysts. The groundmass is holocrystalline and partially altered to chlorite. Dike AK-81-102B is 5 m wide and contains chloritized olivine phenocrysts and large clinopyroxene and plagioclase phenocrysts in a holocrystalline groundmass composed of clinopyroxene, plagioclase, and titano-magnetite.

INTRUSIONS

Three phaneritic intrusive rocks were sampled on Akutan Island. One sample (AK-81-100; app. A) was a piece of float found on Lava Peak, another (AK-81-102; app. A) was collected from a large plug in Sandy Cove, and a third (AK-81-73; app. A) was exposed in the cliff west of Pickup Valley. These three intrusions exhibit different textures.

AK-81-100 is a coarsely crystalline equigranular rock consisting of plagioclase and clinopyroxene. In thin section, the plagioclase and clinopyroxene grains range from 1 to 2 mm (fig. 6a). The subhedral to euhedral shape of the plagioclase and clinopyroxene suggest that the two minerals did not grow in place but were concentrated after most of their growth was completed, possibly by crystal settling in a magma chamber.

In contrast, AK-81-73 (fig. 6b) has an ophitic to subophitic texture that one would expect for a magma crystallizing under static conditions, with clinopyroxene crystallized around plagioclase.

In contrast to the other intrusions, AK-81-102 is a porphyritic rock containing clinopyroxene and plagioclase phenocrysts in a holocrystalline groundmass (fig. 7). The plagioclase contains inclusions of opaque minerals and clinopyroxene and appears to have crystallized after these two mafics nucleated. The clinopyroxene does not contain any inclusions. The groundmass contains plagioclase, clinopyroxene, and an opaque phase.

SUMMARY

Akutan lavas fall into two petrographic groups: the flows and dikes with clinopyroxene and orthopyroxene as the major mafic minerals, and the flows and dikes in which olivine and clinopyroxene are the major mafic minerals. A rare lava type is represented by the hornblende-bearing andesite dikes exposed in Hot Springs Bay Valley. The only flow sampled that was not porphyritic was AK-81-26, from Akutan Harbor. The lack of phenocrysts indicates that this flow was very fluid and may have erupted at a higher temperature (or more quickly) than other flows on the island. The other flows contain individual phenocrysts and crystal clots. The clots are probably the result of crystals clumping together during growth in a magma chamber, or possibly xenocrysts from earlier lavas. There has been some suggestion that crystal clots represent the reequilibration of an amphibolite mantle to lower pressures (Stewart, 1975), but the variety in composition of the crystal clots and the lack of any relic amphibole suggests that this is not the case on Akutan.

The dikes exposed on Akutan Island range from porphyritic to aphanitic, and alteration in these rocks is quite variable. Some of the alteration seen is due to fluids associated with emplacement of the dikes whereas some of the alteration seen may be due to sea-water alteration (D. Hawkins, personal commun.; Mottl and Holland, 1978). This is especially true of those dikes exposed along the coast.

The dikes were examined to determine if they might be related to formation of an older caldera. Significant differences in K-Ar ages of nearby dikes suggests that they are not (Swanson and Romick, 1988).

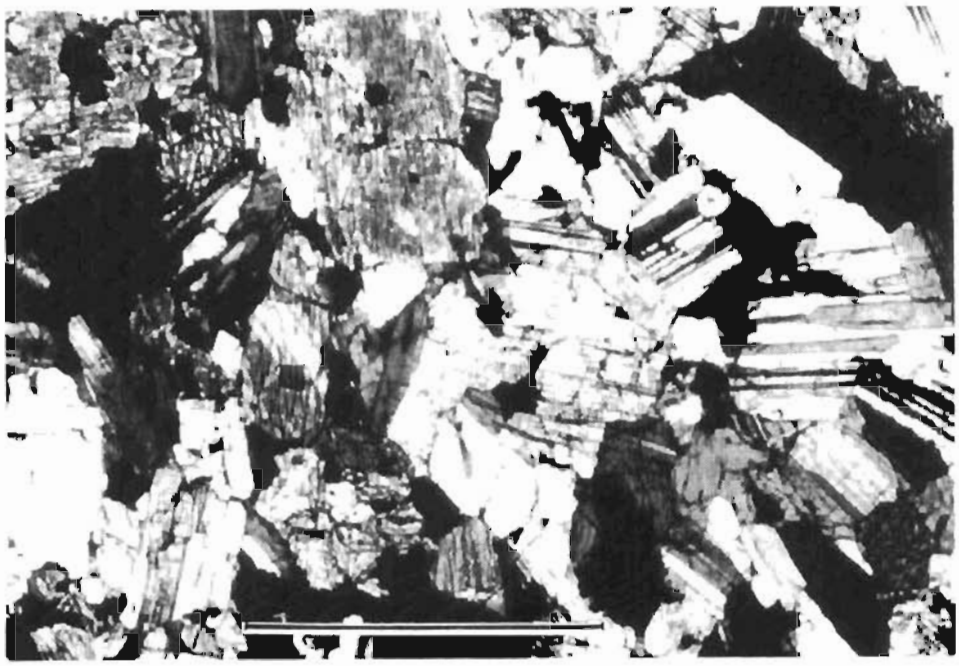

a)

b)

Figure 6. *Photomicrographs of intrusive rocks. (a) Coarse-grained intrusion from western Akutan Island; (b) plagioclase-clinopyroxene gabbro from Hot Springs Bay. Scale = 1 mm.*

MINERALOGY

Akutan lavas are characterized by phenocrysts of plagioclase, clinopyroxene, olivine, orthopyroxene, opaque minerals, and alteration products in a finer grained groundmass. Plagioclase is the only mineral present in all samples.

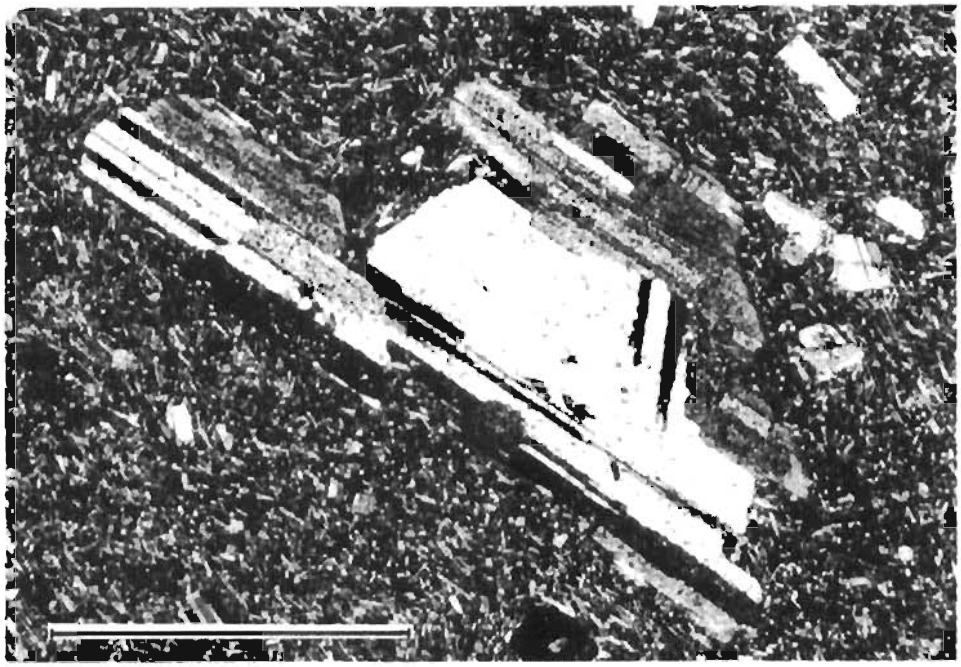

Figure 7. *Photomicrograph of porphyritic intrusion from Sandy Cove. Scale = 1 mm.*

CLINOPYROXENE

Calcium-rich augite is the one type of clinopyroxene present as phenocrysts. Figure 8 shows the results of microprobe analyses of Akutan clinopyroxenes and orthopyroxenes. The clinopyroxene compositions vary about 13 percent ferrosilite (Fs), 8 percent wollastonite (Wo), and 2 percent enstatite (En). The augite from Lava Peak Flows is the most Fs poor, whereas lavas from Hot Springs Bay contain the most Fs. Perfit and Gust's (1981) microprobe analyses of phenocrysts in basalts and andesites are very similar to those analyses reported in this study. Both simple growth twins and polysynthetic twins occur in the clinopyroxenes (fig. 9a, b).

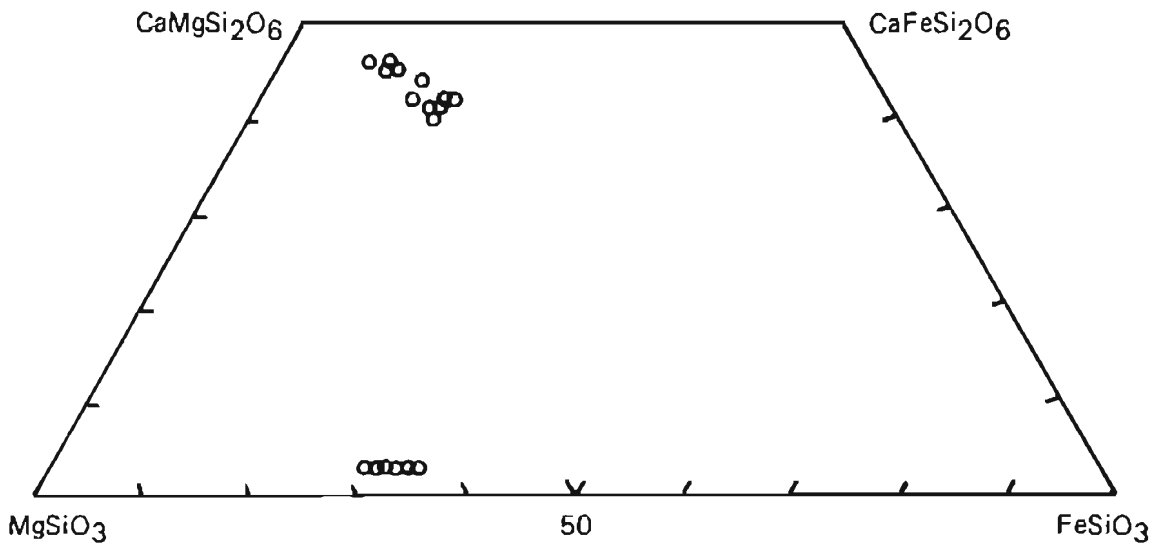

Figure 8. *Plot of microprobe analyses for Akutan clinopyroxenes and orthopyroxenes.*

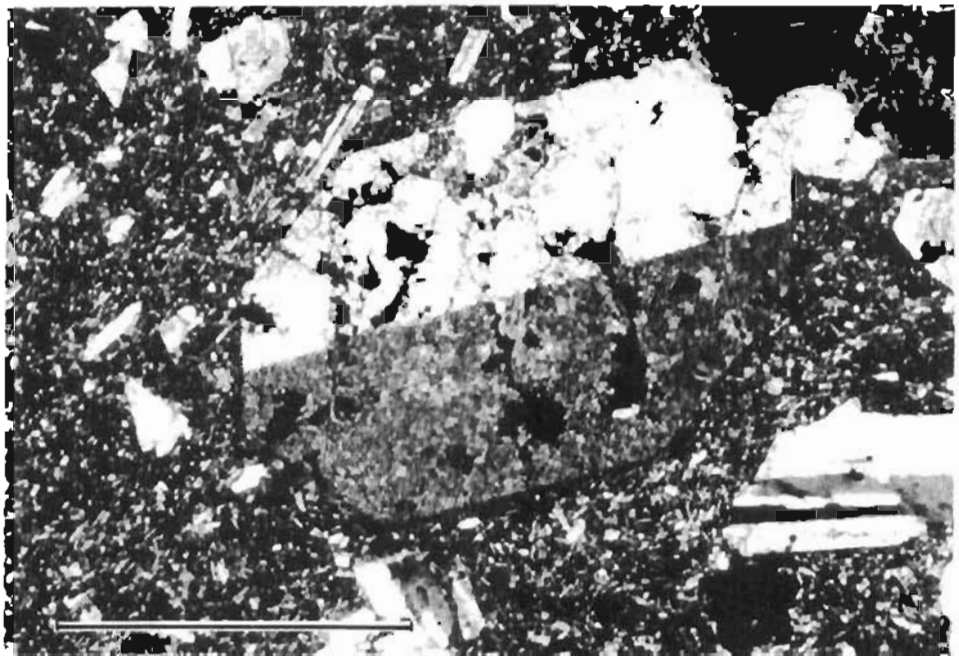

a)

b)

Figure 9. *Photomicrographs of commmon clinopyroxene twinning types. (a) Simple growth twins; (b) polysynthetic twinning (bottom center). Scale = 1 mm.*

There are two texturally distinct populations of clinopyroxene. The first is a group of large anhedral to subhedral phenocrysts up to 7 mm long. These large grains are commonly zoned, but rarely twinned. In contrast, the second population of clinopyroxene consists of smaller subhedral grains that average 0.75 to 1.5 mm in size and are commonly twinned as well as zoned. Both populations occur as individual phenocrysts and as glomerocrysts. The glomerocrysts are up to 8 mm long and usually composed of anhedral grains 0.5 to 2 mm long.

It would be convenient to be able to divide these two dissimilar groups into two generations of growth, the larger grains growing earlier in a relatively undisturbed environment and the smaller phenocrysts growing in a fairly active environment, possibly one with magma erupting. However, there are no compositional differences between the two groups of phenocrysts, which one might expect if they had crystallized at different times.

The clinopyroxenes are biaxial positive with a 2V ranging from 35° to 60°. The large phenocrysts have low birefringence; the small phenocrysts are moderately birefringent. In plain light the clinopyroxenes are pale green and nonpleochroic.

The groundmass pyroxenes are also pale green in plain light, biaxial positive, and have low birefringence. The grains are, in general, too small for 2V determination.

Figure 10 shows well-developed "hourglass" zoning found in Akutan pyroxenes. Most authors ascribe the zoning to different growth rates in different crystallographic directions (Strong, 1969; Gray, 1971; Hollister and Gancarz, 1971; Wass, 1973). The resulting skeletal form is later filled by clinopyroxene richer in FeO, TiO_2, Na_2O, and Al_2O_3. Another type of zoning, not illustrated, appears as an anhedral core surrounded by a euhedral rim. Deer and others (1978) suggest that this type of zoning results from melting the grain during movement of the magma prior to eruption. Thereafter, the temperature drops and a euhedral rim forms around the partially melted crystal (Deer and others, 1978). The zoning indicates that the clinopyroxene was not always in equilibrium with the surrounding liquid. Diffusion of cations within the crystal lattice is not fast enough to allow the crystal composition to readjust in response to the change in liquid composition. The system's response to disequilibrium is to mantle the crystal with a rim that can coexist with the liquid. As the composition of the liquid changes, so does the composition of the rim until crystallization halts the process or the crystal is resorbed.

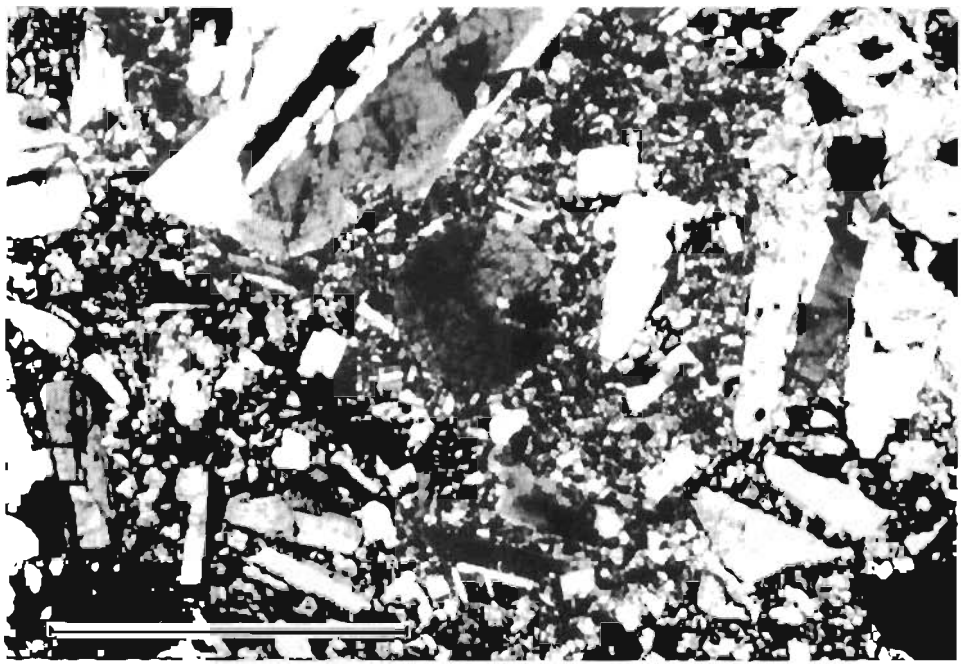

Figure 10. *Photomicrograph of clinopyroxene "hourglass" zoning. Scale* = 1 mm.

ORTHOPYROXENE

The orthopyroxene present in Akutan rocks is hypersthene. The mineral appears in two forms: (1) as euhedral to anhedral phenocripts rimmed by clinopyroxene and (2) as subhedral to anhedral phenocripts without reaction rims. The two textural types may occur in the same rock, and microprobe analyses indicate that there is little compositional difference between them (app. B). There is lime difference in composition between then augite rimming the hyperothene and augite as independent phenocrysts.

The hypersthene phenocrysts are 0.5 to 0.75 mm long, biaxial negative with a 2V between 55° and 70°, and have low birefringence. The phenocrysts have pale pink to yellow to green pleochroism.

OLIVINE

Olivine never makes up more than 8 percent of the rock when it is present, and usually makes up only 2 to 4 percent. It is generally subhedral and anhedral in form, commonly occurring as fragments of grains. Occasionally euhedral olivine is present, and skeletal varieties are common in some of the western flows. The phenocrysts are rarely greater than 1 mm in diam. The olivine commonly has an oxidized outer rim or is partially altered to iddingsite. The olivine has high relief, moderate to high birefringence, and is clear in plain light. Zoning is either very weak or nonexistent. The skeletal variety analyzed by microprobe in figure 11 have a compositional range between FO_{75} and FO_{69}. Figure 11 also shows the microprobe results from Perfit and Gust (1981); for rocks containing only olivine and clinopyroxene, their data closely compare with these of this study although some of their analyses have values up to FO_{90}.

PLAGIOCLASE

Plagioclase is the most abundant mineral in Akutan lavas. It is present as phenocrysts and in the groundmass of all of the flows and dikes examined. Plagioclase makes up 8 to 44 percent of lavas and may make up to 100 percent of the phenocrysts present in a particular rock. Plagioclase phenocrysts range from 0.5 to 7 mm long. Inclusions of glass, clinopyroxene, and opaque minerals are occasionally present.

Plagioclase phenocrysts are generally subhedral to euhedral, although there are anhedral fragments present. Normal, oscillatory, and reversed zoning are present in Akutan plagioclase. Twinning is ubiquitous, and albite and carlsbad twins are the most common types. Cruciform penetration twins are seen occasionally.

Figure 12 shows the type of compositional zoning present in samples from Akutan Island. Microprobe data for the Lava Peak Flows show the plagioclase to be very calcic (An_{90} to An_{80} core values) and zoned 10 percent anorthite between core and rim. These plagioclase are normally zoned, where anorthite content decreases from core to rim, but occasionally have oscillatory zoning, where rim and core are about equal in anorthite content and the intermediate interior more sodic.

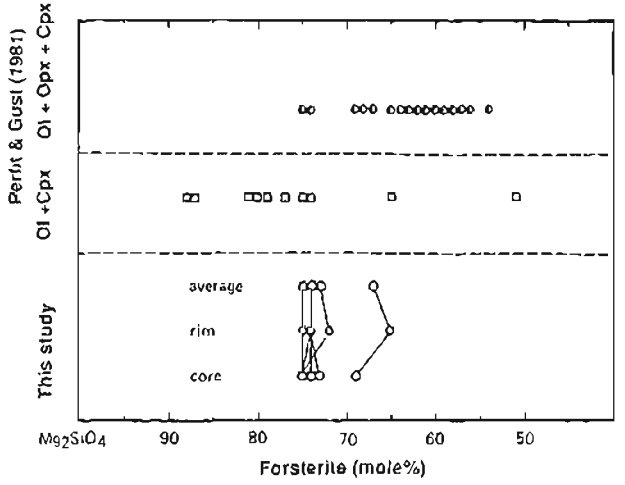

Figure 11. *Diagram showing microprobe analyses of olivine phenocrysts. Also included are analyses from Perfit and Gust (1981). Open circles represent analyses from this study; half filled circles represents analyses from Perfit and Gust (1981) where olivine exists in orthopyroxene and clinopyroxene; and open squares represents olivine analyses (Perfit and Gust's, 1981) where olivine exists with clinopyroxene only.*

Figure 12. *Diagram showing microprobe analyses of plagioclase phenocrysts. Open circle = core; open square = rim; solid circle = intermediate values.*

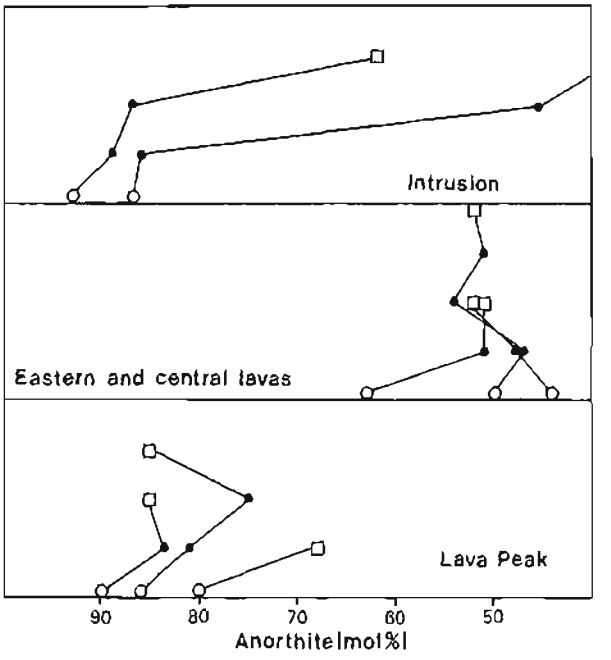

Plagioclase from Hot Springs Bay lavas are more albitic and show less zoning. One sample is zoned between An_{45} and An_{50}, whereas another zoned 1 percent between An_{50} and An_{51}.

Sample AK-81-73 is from a gabbroic intrusive on the west side of Hot Springs Bay. The plagioclase from this sample shows extreme zoning. One phenocryst is zoned between An_{93} and An_{60}, whereas another zoned from An_{87} to An_{1} midway to the rim, with an outer rim of alkali feldspar.

The division between the Lava Peak flows and the other lavas seen in the microprobe data may reflect the number of samples analyzed, rather than a real difference. More analyses are needed to confirm the apparent separation of values.

Figure 13a and b show the variety of glass inclusions present in plagioclase phenocrysts. They occur as a fine dusting in the core, at some intermediate point between core and rim, in the rim, or at some combination of the three. The zone of inclusions is usually parallel to the crystal boundaries. In some cases the inclusions are not oriented with respect to the crystal faces and appear as irregularly shaped blebs in the interior of the phenocryst. The textures shown in figure 13a and b indicate a change in the conditions of crystal growth. This change may correspond to conditions of higher undercooling, possibly caused by changes in temperature or pressure. Undercooling is the difference between the liquidus temperature of the crystal and the temperature of the liquid that the crystal is growing in. As the degree of undercooling increases, crystal growth changes from planar to skeletal (Lofgren, 1980). High growth rate, combined with the skeletal crystal form, may make it possible for the crystal to trap liquid as it grows. The trapped liquid is quenched to a glass. A change to lower undercoolings would result in a return to planar crystal boundary growth and the euhedral outline seen on Akutan plagioclase.

Other types of inclusions include large amounts of brown glass trapped in the interior of plagioclase grains, and clinopyroxene and opaque grains that appear to have been trapped in the plagioclase as it crystallized.

The plagioclase in samples AK-81-73 and -100, both coarse grained intrusions, are essentially inclusion free. Emplacement at depth would cause gradual cooling, resulting in crystallization at low undercooling. This in turn would cause planar crystal boundary growth. The slow cooling rate would also result in low growth rates, which would not allow glass to be trapped within plagioclase phenocrysts.

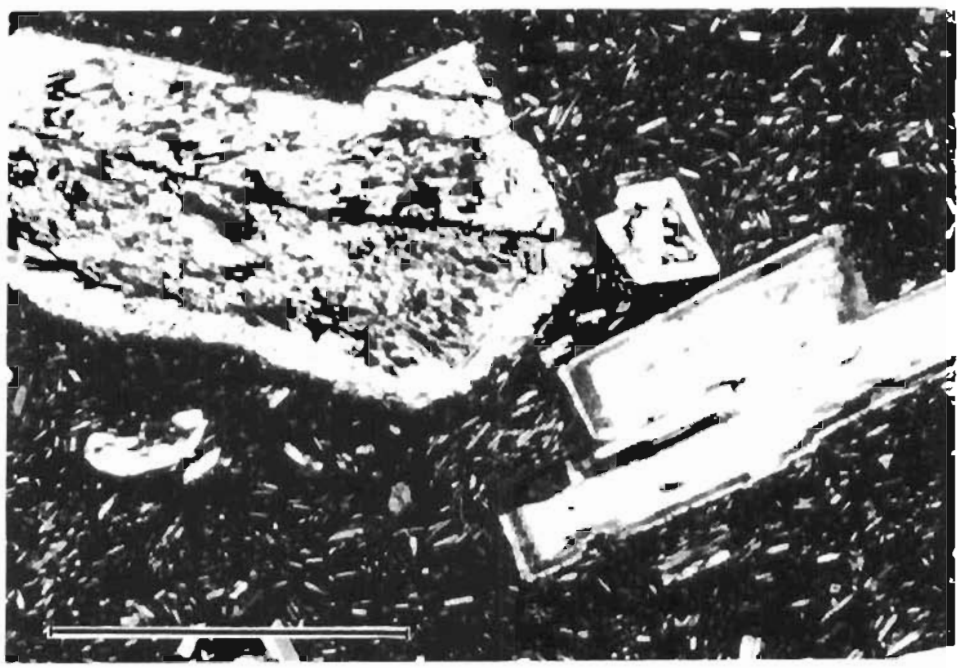

a)

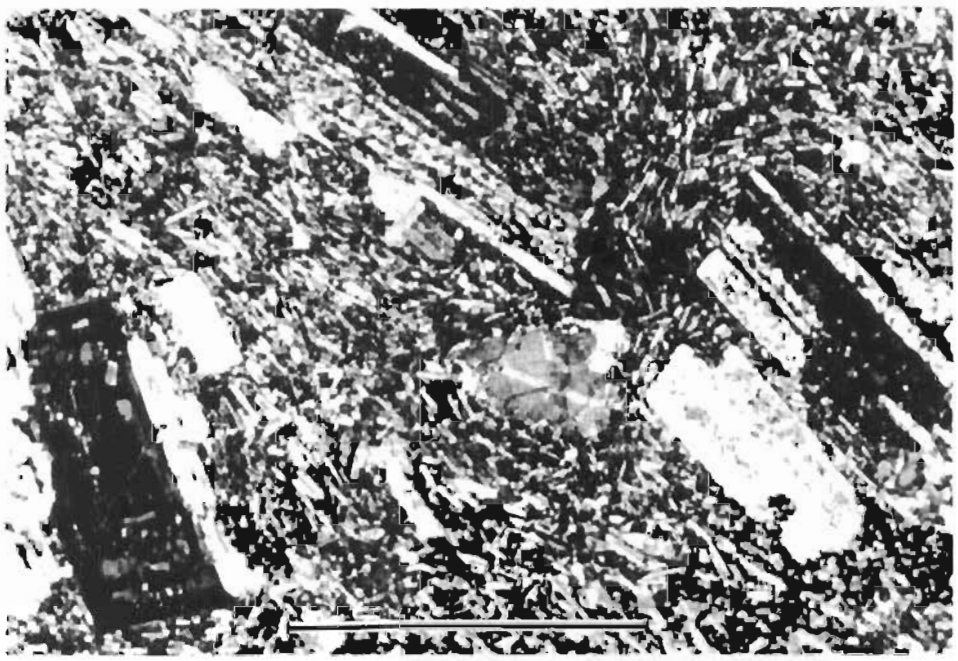

b)

Figure 13. *Photomicrographs of inclusions in plagioclase phenocrysts. (a) Glass inclusions parallel to the margins of the crystal and brown glass in the interior of the crystal; (b) opaque minerals and clinopyroxene within the crystal. Scale = 1 mm.*

ACCESSORY AND ALTERATION MINERALS

OPAQUE MINERALS

Opaque phenocrysts generally make up less than 1 percent of Akutan lavas. Oxides are usually restricted to the groundmass. Those present as phenocrysts are subhedral to anhedral and less than 0.75 mm in diameter. Skeletal varieties observed in some samples probably crystallized late in the history of the magma. The opaque minerals were occasionally seen as in clusions in angite and hypersthene phenocrysts, and rarely in olivine and plagioclase. Some euhedral forms are present and usually appear as cubes or octahedrons, suggesting they are some type of magnetite. Opaque minerals, when present in the groundmass, are usually euhedral to subhedral and about the same size (0.1 to 0.2 mm) as other minerals present.

HORNBLENDE

Hornblende is present in two samples, both dikes from Hot Springs Bay Valley. The amphibole has olive- to light-green pleochroism (X - yellow-green, Y - brownish-green, and Z - green) and moderate birefringence; it is anhedral and 0.25 to 1.5 mm in diameter. Hornblende never makes up more than 1 percent of the rock.

APATITE

Apatite occurs as euhedral rods in plagioclase. It is about 0.1 mm long and occurs in trace amounts in most of the rocks examined.

CARBONATE

Carbonate is a common alteration mineral in the older lavas on Akutan. It is a common vesicle filling and alteration product of mafic minerals and groundmass, and occasionally replaces plagioclase. The carbonate is uniaxial negative, has variable relief, is clear in plain light, and has very high birefringence. The grain size is quite variable, ranging from microcrystalline to 4 mm in diameter.

CHLORITE

Chlorite is the most common alteration product of Akutan lavas. It has moderate birefringence and occurs as microcrystalline grains with light to dark-green and to medium-yellow pleochroism. Chlorite may make up 10 percent of the rock and commonly occurs as pseudomorphs of olivine and clinopyroxene. It sometimes occurs as a lining in amygdules where carbonate fills the interior of the amygdule.

QUARTZ

Quartz is occasionally present as an alteration mineral and usually occurs in veinlets associated with carbonate. It occurs in trace amounts and is less than 0.25 mm in size.

SERPENTINE MINERALS

Olivine is rarely altered to a nonpleochroic serpentine mineral. It is fibrous, has low birefringence low relief, and occurs as pseudomorphs after olivine.

CRYSTALLIZATION SEQUENCE

Table 4 shows the crystallization sequence for Akutan lavas. Generally, plagioclase is the first mineral to crystallize. Opaque minerals occasionally crystallize before plagioclase (Marsh, 1976), as in samples AK-81-20, -34, -38, and -62, but usually crystallize after nucleation of plagioclase and are seen enclosed by olivine and clinopyroxene. Clinopyroxene appears to follow olivine in the crystallization sequence. This is indicated by the presence of basalts

Table 4. *Crystallization sequence for Akutan lavas*

Location	Sample	Crystallization sequence from left to right
Lava Peak(D)	AK-81-1	Plag-Opq-Ol-Cpx-GM
Lava Peak(U)	AK-81-2	Plag-Opq-Ol-Cpx-GM
Lava Peak(U)	AK-81-3	Plag-Opq-Ol-Cpx-GM
Lava Peak(U)	AK-81-4	Plag-Opq-Ol-Cpx-GM
Lava Peak(L)	AK-81-5	Plag-Opq-Ol-Cpx-GM
Lava Peak(L)	AK-81-6	Plag-Opq-Ol-Cpx-GM
Lava Peak(L)	AK-81-7	Plag-Opq-Ol-Cpx-GM
Lava Peak(L)	AK-81-8	Plag-Opq-Ol-Cpx-GM
Lava Peak(L)	AK-81-9	Plag-Opq-Ol-Cpx-GM
Lava Peak(L)	AK-81-10	Plag-Opq-Ol-Cpx-GM
Lava Peak(L)	AK-81-11	Plag-Opq-Ol-Cpx-GM
Lava Peak(L)	AK-81-12	Plag-Opq-Ol-Cpx-GM
Lava Peak(L)	AK-81-13	Plag-Opq-Ol-Cpx-GM
Lava Peak(L)	AK-81-14	Plag-Opq-Ol-Cpx-GM
Lava Peak(L)	AK-81-15	Plag-Opq-Ol-Cpx-GM
Old flow	AK-81-16	Plag-Opq-Ol-Cpx-GM
Old flow	AK-81-17	Plag-Opq-Ol+Opx-Cpx-GM
Old flow	AK-81-18	Plag-Opq-Ol-Opx-Cpx-GM
Old flow	AK-81-31	Plag-Ol-GM
Old flow(D)	AK-81-32	Plag-GM
1978 flow	AK-81-27	Plag-Opx-Cpx-GM
Pre-1870 flow	AK-81-35	Plag-Opq-Cpx-GM
Float	AK-81-100	Plag-Cpx
Open Bight	AK-81-51	Opq-Cpx+Plag-GM
Open Bight	AK-81-52	Plag-Opq-Cpx-GM
Pickup Valley	AK-81-21	Opq-Plag-Cpx-GM
Pickup Valley	AK-81-22	Plag-Opq-Cpx-GM
Pickup Valley	AK-81-23	Plag-Opq-Opx-Cpx-GM
Pickup Valley	AK-81-24	Ol+Plag-Cpx-GM
Cow Point(D)	AK-81-54A	Plag-Opq-Cpx-GM
Cow Point(D)	AK-81-57A	Opq-Plag-GM
Cow Point(D)	AK-81-57B	Plag-Opq-Cpx-GM
HSB Valley(D)	AK-81-38	Plag-Cpx-GM
HSB Valley(D)	AK-81-43	Plag-Cpx-Hb-GM
HSB Valley(D)	AK-81-50	Plag-Cpx-Cpx+GM
HSB Valley(D)	AK-81-61	Plag-Opq-Ol-GM
HSB Valley(D)	AK-81-70	Ol-Plag-Cpx-GM
HSB Valley(D)	AK-81-71	Plag-Opx-Hb-GM
HSB Valley(F)	AK-81-62	Plag-Opq-Cpx-GM
HSB Valley(F)	AK-81-65	Ol-Cpx-Plag-GM
HSB Valley(F)	AK-81-69	Plag-Opq-Ol-GM
West HSB Valley(I)	AK-81-73	Opq-Plag-Cpx
Sandy Cove(I)	AK-81-102	Opq-Cpx-Plag

D - dike, U - upper series, L - lower series, HSB Valley - Hot Springs Bay Valley, F - lava flow, I - intrusion, Plag - plagioclase, Opq - opaque, Ol = olivine, Cpx - clinopyroxene, GM - groundmass, Opx - orthopyroxene, Hb - hornblende.

which contain plagioclase, opaque minerals, olivine, and clinopyroxene, but no orthopyroxene. In samples where olivine is absent, orthopyroxene is usually present. Skeletal olivine (in the basalts) and hornblende (in the andesites and dacites) are the last minerals to form. A generalized crystallization sequence for Akutan lavas is: (1) plagioclase, (2) plagioclase + oxides, (3) plagioclase + oxides + olivine, (4) plagioclase + oxides + olivine + clinopyroxene, (5) plagioclase + oxides + clinopyroxene + orthopyroxene, and (6) plagioclase + oxides + clinopyroxene + hornblende. Although there is no experimental data on the crystallization of Akutan lavas, work done on Atka basalts by Baker and Eggler (1983) at various pressures reproduces the crystallization sequence described above for magmas that crystallized at less than 8 kb pressure. The early or late appearance of opaque minerals depended on the oxygen fugacity of the system. Thus, the sequence based on textural relationships appears in Akutan basalts and andesites appears to be consistent with experimental work on rocks of similar composition.

SUMMARY

Mafic mineral compositions on Akutan are remarkably uniform, suggesting that whatever changes have occurred in the magmas that formed Akutan lavas, the factors influencing mineral composition (pressure, temperature, P_{H2O}, liquid composition, etc.) remained fairly constant. Unalaska Island, Frosty Peak Volcano, and Adak Island pyroxenes and plagioclase are very similar in composition to Akutan minerals (Byers, 1959; Drewes and others, 1961; Marsh, 1976; Perfit and Gust, 1981), which suggests that the lavas for many Aleutian volcanoes are similar in composition and form minerals of similar composition.

What is variable on Akutan is the relative abundance of particular minerals. Olivine is abundant in Lava Peak rocks, whereas orthopyroxene is more abundant in some of the Hot Springs Bay lavas. Plagioclase and clinopyroxene are the only ubiquitous minerals in Akutan lavas.

GEOCHEMISTRY

MAJOR OXIDES

Appendix C lists the whole rock major-oxide analyses. Oxide totals ranged from 98.52 to 100.71 percent. Harker variation diagrams are shown in figure 14. MgO, FeO, and CaO decrease with increasing SiO_2, whereas Na_2O and K_2O generally increase with increasing SiO_2. Curves for TiO_2 and Al_2O_3 are flat with respect to SiO_2, and Fe_2O_3 data are too dispersed to draw conclusions regarding a particular trend. The relative merits of these plots versus plots of more complex ratios are discussed by Cox and others (1979) and Maaloe and Peterson (1981). Samples from Lava Peak and from the other parts of the island do not plot as separate groups on the Harker diagrams.

These diagrams are supposed to represent the "liquid line of descent" of a fractionating magma. As certain elements are incorporated into early- forming minerals, their concentration in the remaining liquid decreases, whereas those elements not used in the minerals increase in abundance. These trends, whether increasing or decreasing, indicate changes in the liquid composition as it fractionates. Ideally, one should use analyses from glasses (quenched liquid) to obtain accurate measurements of composition; however, this is rarely possible. Most volcanics are crystallized to some degree, and many are porphyritic. The local addition or subtraction of phenocrysts in these rocks may significantly affect where samples plot on the trends, although porphyritic rocks may still represent liquid compositions. If, for instance, olivine crystals settle toward the bottom of a cooling flow, that part will be enriched in olivine. And if a sample is taken from that part of the flow and analyzed it will plot above the trends for FeO and MgO because it has been enriched in those components by the addition of olivine. Likewise, samples taken from the part of the flow depleted in olivine will plot below the trends because they are depleted in the two oxides because of the removal of olivine. If many of the samples analyzed are porphyritic, considerable scatter in the trends can occur because of the above effect. This may be the case for Akutan samples. Partial alteration of some of the samples may also affect the analyses by preferentially adding or subtracting certain elements.

Oxide-oxide plots were constructed to see if any distinction could be drawn between the Lava Peak rocks and the other lavas on the island. The results are shown in figures 15 through 18. Again, no clear distinction can be made between the Lava Peak volcanics and other volcanics on Akutan Island. The fact that the two groups of lavas do not plot as separate trends suggests that they were not derived from different parental magmas or significantly different sources.

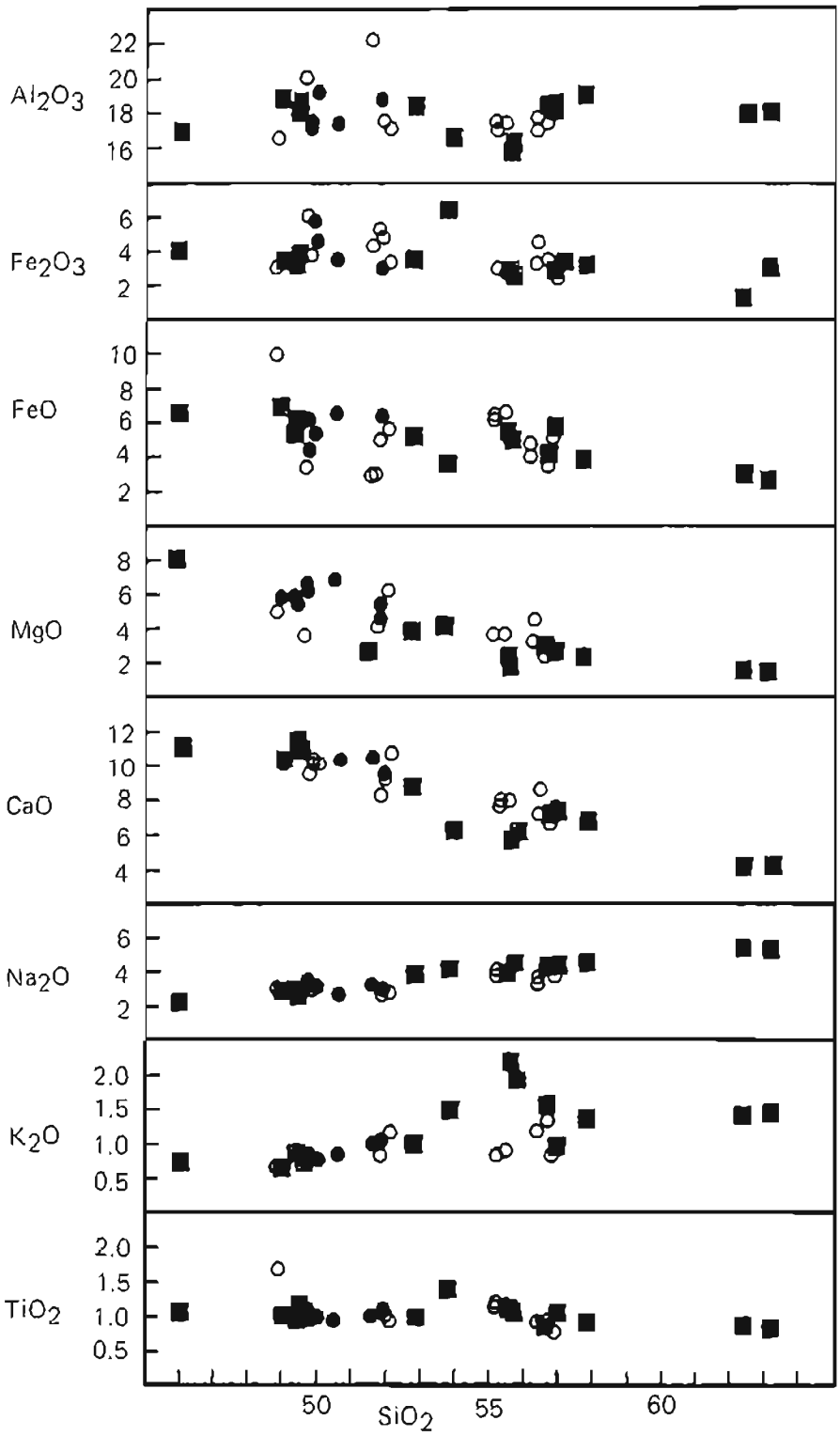

Figure 14. *Harker variation diagram. Solid circle = Lava Peak basalts; open circle = other modern lavas; solid square = eastern lavas. Amounts are in weight-percent.*

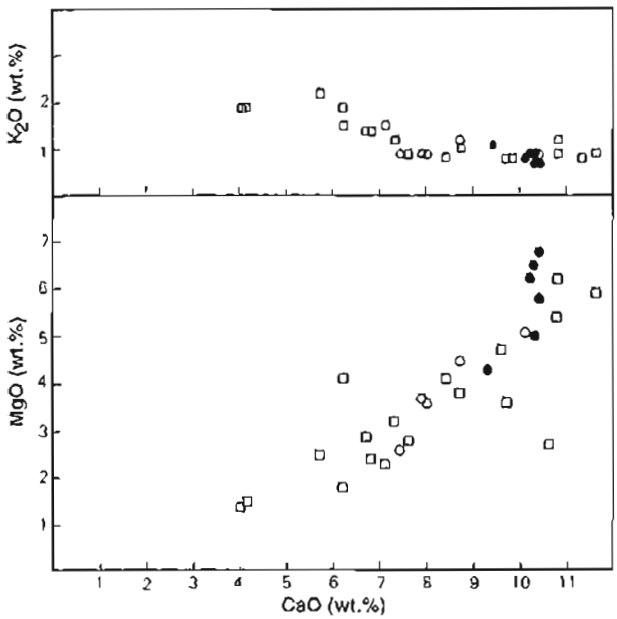

Figure 15. *MgO-CaO and K_2O-CaO plots of Akutan samples. Open circle = western lavas; solid circle = Lava Peak basalts; solid square = eastern lavas.*

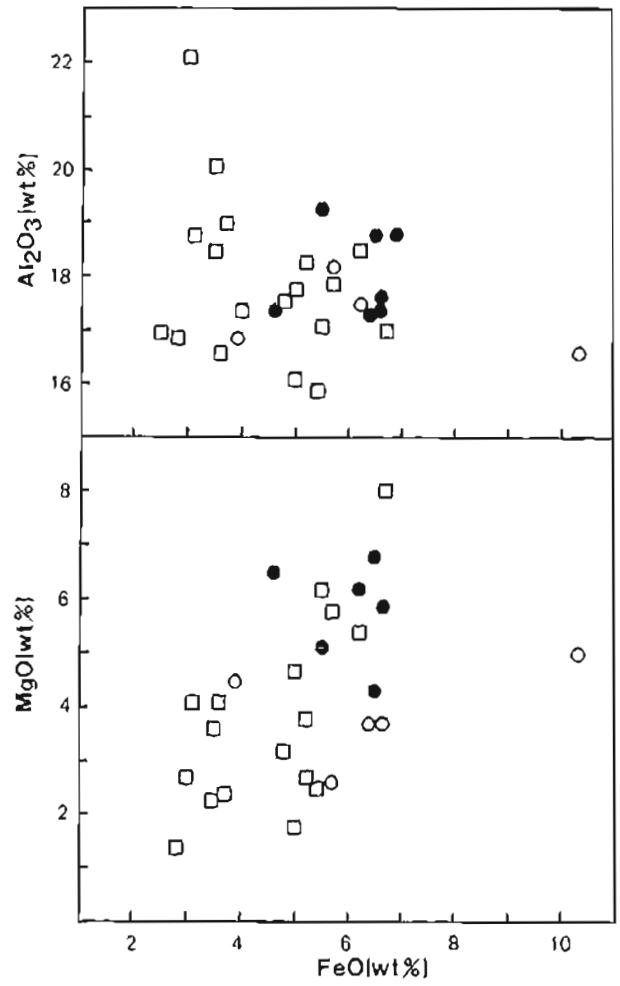

Figure 16. *MgO-FeO and Al_2O_3-FeO plots of Akutan samples. Open circle = western lavas; solid circle = Lava Peak basalts; solid square = eastern lavas.*

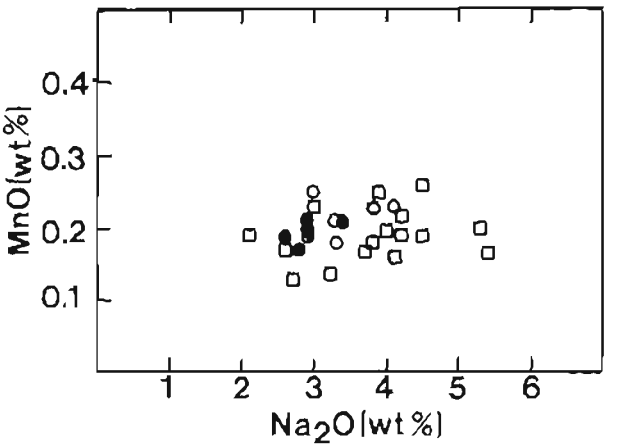

Figure 17. *Na_2O-MnO plots of Akutan samples. Open circle = western lavas; solid circle = Lava Peak basalts; solid square eastern lavas.*

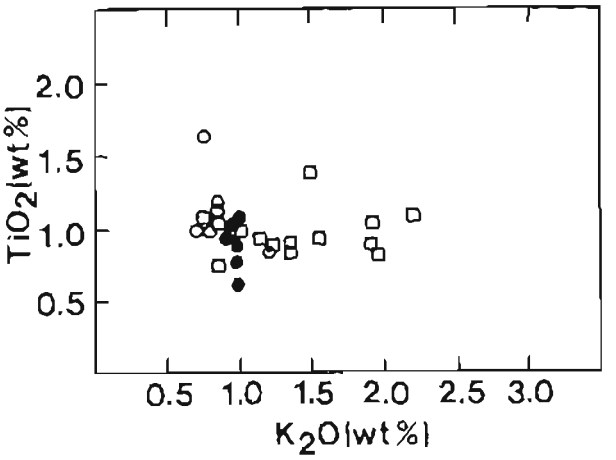

Figure 18. *TiO_2-K_2O plots of Akutan samples. Open circle = western lavas; solid circle = Lava Peak basalts; solid square eastern lavas.*

An AFM diagram (fig. 19) shows a slight iron enrichment similar to other plots of Aleutian rocks (Marsh, 1976). The FeO*/MgO versus SiO_2 diagram (fig. 20) also shows the mild iron-enrichment trend typical of Aleutian tholeiites as defined by Kay and others (1982). Marsh (1976) noted that Aleutian trends were higher in iron enrichment than the trend for Cascade rocks, but lower than the trend for Tongan volcanics. Again, the lava Peak rocks and the other lavas intermix on the diagram. In a plot of total alkalis (K_2O+Na_2O) versus SiO_2 (fig. 21), Akutan rocks fall in the high-alumina field as defined by Kuno (1966). Perfit (1978) suggests that it is possible to derive these high-alumina rocks from high-magnesium basalts found on Akutan Island.

The effect of fractionation of plagioclase, olivine, and augite can be seen in figure 22. As the magma(s) differentiated, the CaO/Al_2O_3 ratio decreased and the FeO*/MgO ratio increased. This is due to the precipitation of early-forming calcic plagioclase and magnesian olivine and augite, which left the remaining liquid enriched in FeO and depleted in CaO and MgO.

STATISTICAL ANALYSES

The oxide data were analyzed by two multivariate statistical methods to see if more sophisticated techniques could distinguish the two petrographic groups. The oxide data were analyzed by cluster analysis (McCammon and Wenninger, 1970), and then a stepwise multiple discriminant analysis (Jennrich and Sampson, 1981). A dendrograph (McCammon and Wenniger, 1970), obtained from the cluster analysis, is shown in figure 23.

Cluster analysis separates samples into groups (or clusters) on the basis of measured variables. The number of clusters that result from the analysis are not known beforehand, and samples are generally free to enter any cluster that develops. In contrast, discriminant analysis requires the number of groups to be set before analysis, with each sample assigned to a particular group (Davis, 1973). By minimizing the within-group variance and maximizing the between-

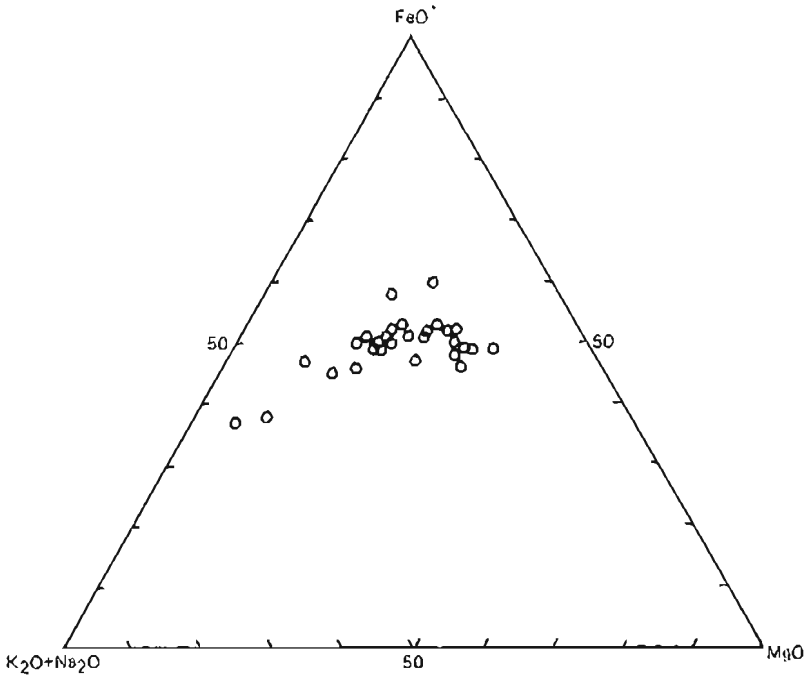

Figure 19. *AFM diagram for Akutan samples.*

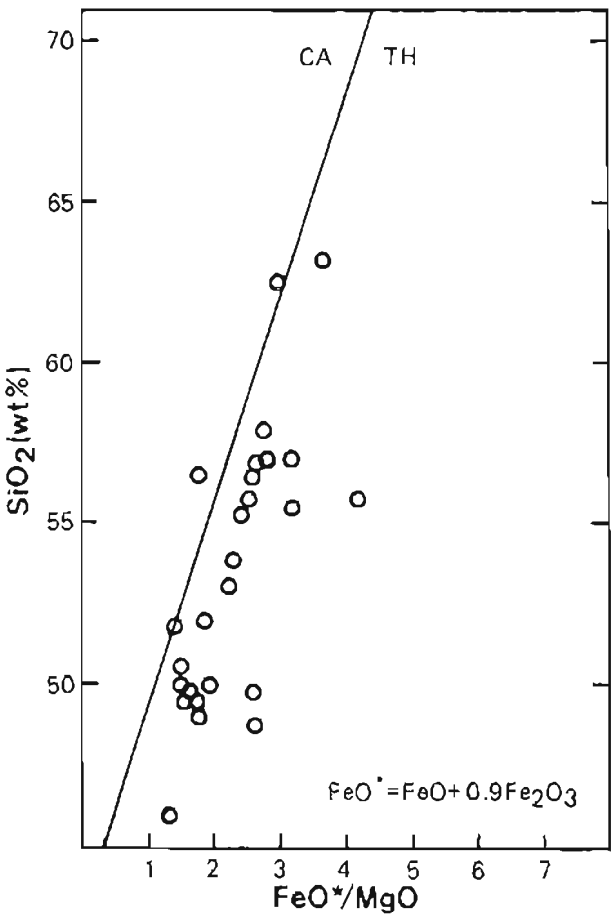

Figure 20. *SiO_2 versus FeO*/MgO diagram for Akutan samples. Diagram from Miyashiro (1974).*

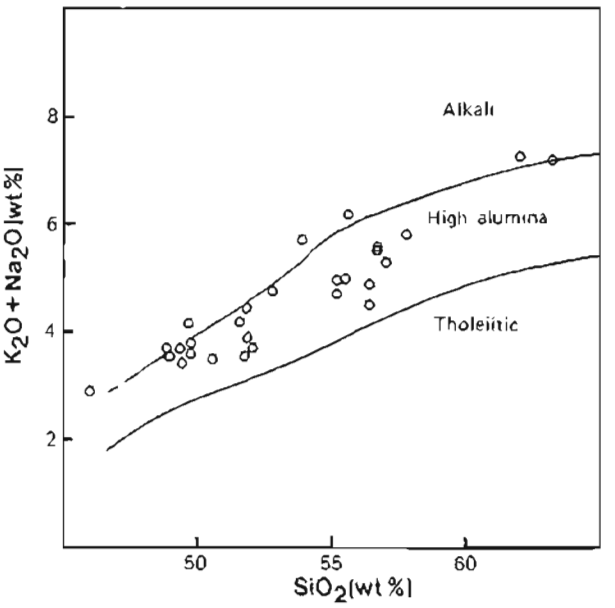

Figure 21. *Total alkalis versus silica diagram from Kuno (1966). Akutan lavas fall in the high-alumina field.*

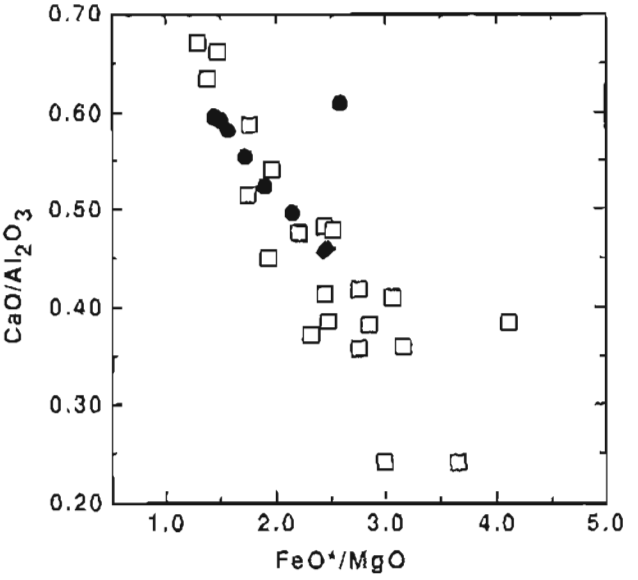

Figure 22. *CaO/Al_2O_3 versus FeO^*/MgO diagram showing CaO and MgO fractionation in Akutan lavas. Solid circle = Lava Peak + western lavas; solid diamonds = modern Akutan Volcano; open square = eastern lavas.*

group variance, the discriminant analysis identifies the variables, that distinguish the groups. Stepwise multiple discriminant analysis constructs a linear equation for each group by going through a series of simple analyses that move from one analysis to the next by adding or subtracting a classification variable along the way (Jennrich, 1977).

The cluster analysis distinguished four general groups of lavas (fig. 23). The stepwise discriminant analysis used P_2O_5 and TiO_2 to identify the four groups. The discriminant functions for the four groups are listed below and in appendix D. (P_2O_5 and TiO_2 are in weight-percent and X is the value of the discriminant.)

WestF	$X = 100.33TiO_2 + 264.09P_2O_5 - 83.22$
EastF	$X = 93.55TiO_2 + 245.03P_2O_5 - 72.26$
WestD	$X = 151.90TiO_2 + 414.89P_2O_5 - 194.84$
EastD	$X = 125.68TiO_2 + 343.05P_2O_5 - 133.74$

With multiple discriminant analysis we had difficulty distinguishing the two groups of flows defined by the cluster analysis. Samples classified as EastF by the cluster analysis were classified as WestF by the discriminant analysis and

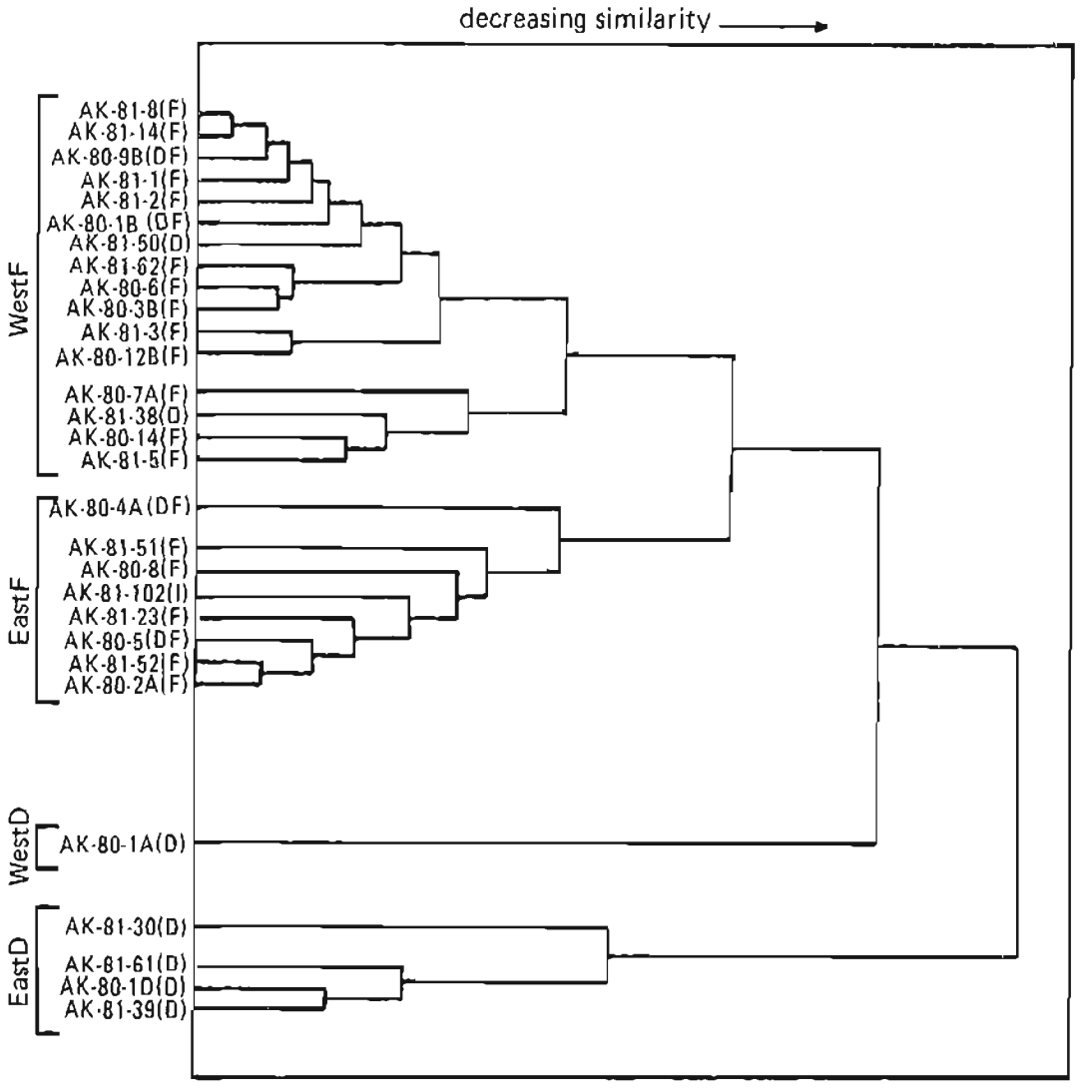

Figure 23. *Dendrograph plot of Akutan lava flows and dikes. D - dikes, F - lava flows, I - intrusions, DF - debris-flow deposits.*

vice versa. Table 5 lists the posterior probabilities for the two groups of flows. The probablities represent the chance that any particular analysis will be classified in a particular group. A high probability in one group is needed for a clear classification. Most of the flows listed in table 6 could be classified into either group.

A canonical plot of the groups and their means is the best two-dimensional display of the relationships between the four groups (fig. 24). The two groups of flows have only slight differences between their means.

Both groups of dikes plot well away from either group of lava flows. Both partially altered and unaltered dikes plotted together indicating that the difference between the flows and dikes is a real phenomenon and not a result of alteration. Two dikes (AK-81-50, -38) plot with the lava flows.

The statistical analyses also suggest that the lava flows on Akutan Island are chemically similar and are difficult to distinguish on the basis of major-element chemistry. The cluster analysis grouped Lava Peak flows with flows from other parts of the island. The discriminate analysis permitted some rearrangement of the groups but it also could not distinguish the two petrographic groups.

Table 5. *Posterior probabilities for the four groups of lavas distinguished by cluster analysis*

[The classifications are those assigned by the multiple discriminant analysis. The original classification was taken from the groups identified by the cluster analysis (fig. 26). Seven samples were run as unknowns to see if the multiple discriminant analysis would place them in more appropriate groups than the ones they were originally in.]

Sample	Class.	EastF	WestF	WestD	EastD
AK-81-5	WestF	0.651	0.347	–	–
AK-81-50	WestF	0.532	0.468	–	–
AK-80-4a	WestF	0.735	0.249	–	–
AK-81-62	WestF	0.704	0.165	–	0.131
AK-80-1b	WestF	0.731	0.175	–	–
AK-80-9b	WestF	0.762	0.221	–	–
AK-80-12b	WestF	0.532	0.468	–	–
AK-80-3b	WestF	0.566	0.433	–	–
AK-80-7a	WestF	0.651	0.345	–	–
AK-80-8	WestF	0.655	0.341	–	–
AK-81-1	EastF	0.348	0.652	–	–
AK-81-2	EastF	0.397	0.602	–	–
AK-81-3	EastF	0.457	0.603	–	–
AK-81-8	EastF	0.376	0.624	–	–
AK-81-14	EastF	0.439	0.561	–	–
AK-80-5	EastF	0.442	0.558	–	–
AK-81-23	EastF	0.320	0.680	–	–
AK-81-51	EastF	0.313	0.687	–	–
AK-81-52	EastF	0.364	0.636	–	–
AK-81-102	EastF	0.240	0.760	–	–
AK-80-5	EastF	0.452	0.548	–	–
AK-8-2a	EastF	0.276	0.724	–	–
AK-80-1a	WestD	–	–	0.998	0.002
AK-80-14	EastD	0.301	0.031	–	0.668
AK-81-30	EastD	–	–	0.046	0.954
AK-81-61	EastD	0.054	0.004	–	0.942
AK-80-1d	EastD	–	–	0.005	0.995
AK-81-38	EastD	0.025	0.001	–	0.973
AK-81-39	EastD	0.008	–	–	0.991

WestF - west flows, EastF - east flows, WestD - west dikes, EastD - east dikes.

Table 6. *Geothermometry for Akutan mineral pairs*

Sample	Mineral pair	Temp	Temp at 5 kb (°C)	Temp at 10 kb (°C)	Temp at 15 kb (°C)
AK-81-23	Opx-Cpx	1180[a]	–	–	–
		1185[a]	–	–	–
		1070[b]	–	–	–
		1068[b]	–	–	–
AK-81-1	Ol-Cpx	992[c]	1020	1044	1075
		1009[c]	1037	1063	1090
AK-81-10	Ol-Cpx	1015[c]	1042	1068	1095
		1012[c]	1039	1066	1092

Opx - orthopyroxene, Cpx - clinopyroxene, Ol - olivine.
[a]Wood and Banno (1973) geothermometer.
[b]Wells (1977) geothermometer.
[c]At 1 bar pressure.

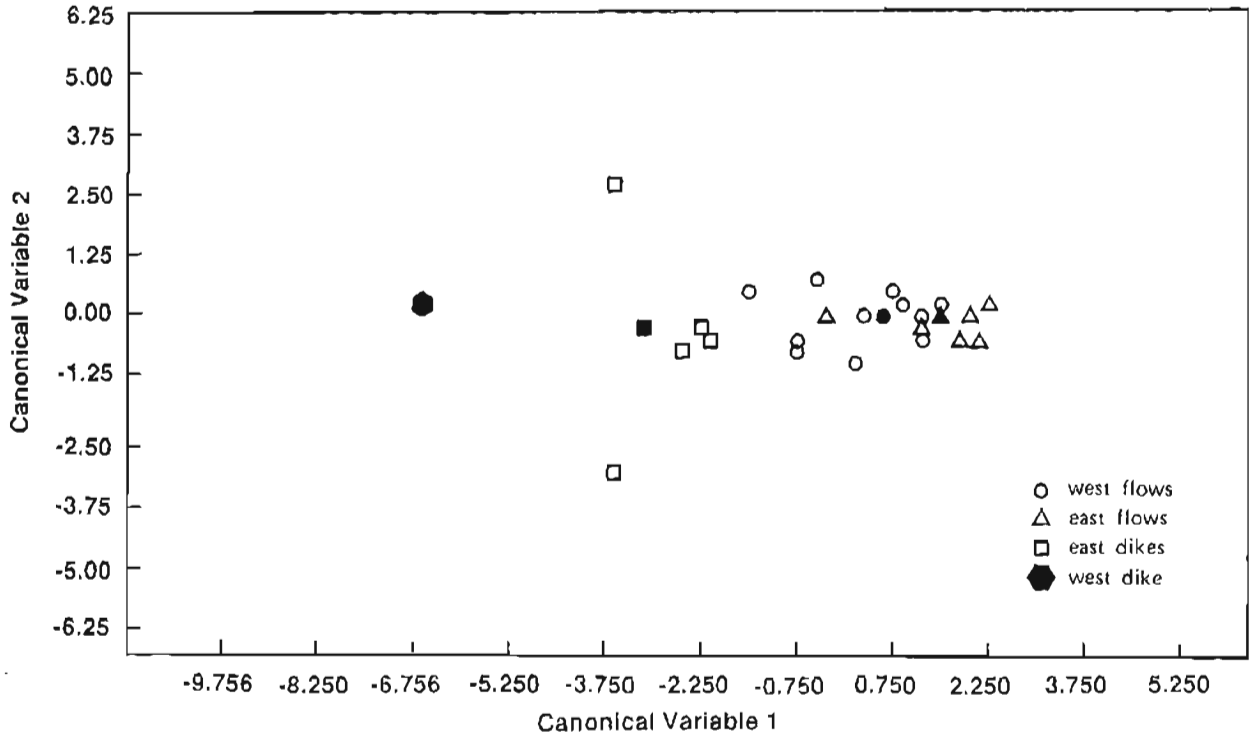

Figure 24. *Canonical plot of groups, group means, and samples. Solid symbols represent the group means.*

NORMATIVE MINERALOGY

Appendix C lists the normative mineralogy for the 31 samples from Akutan. All of the rocks contain normative hypersthene, which by definition must be present in tholeiitic rocks (Cox and others, 1979). Most of the rocks are quartz normative. Five samples are olivine normative and their geographic distribution does not follow any pattern across the island. Lava Peak flows range from slightly olivine normative at the bottom to quartz normative farther up the sequence. They also have greater than 11 percent normative hypersthene, while the other volcanics generally do not (fig. 25).

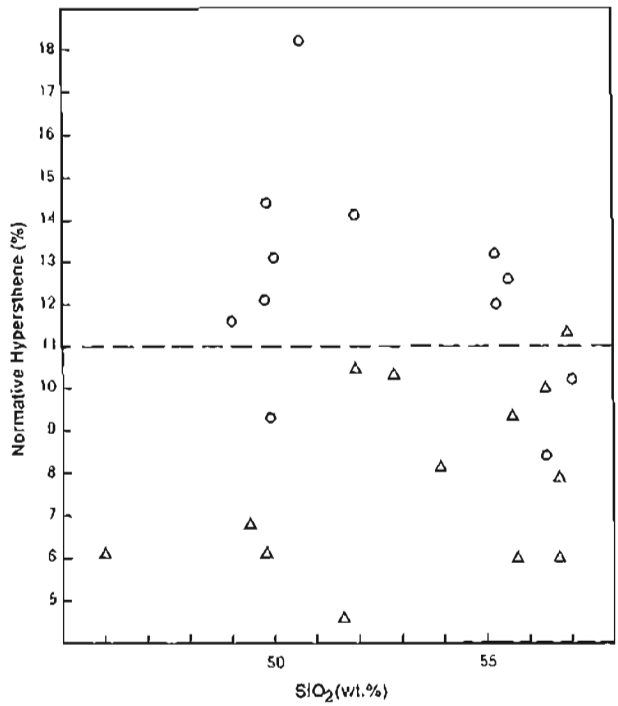

Figure 25. *Normative hypersthene versus SiO_2. Triangles = eastern lavas; circles = western lavas.*

RB AND SR ANALYSES

Figure 26 is a plot of Sr versus Rb igneous rocks from Unalaska (Perfit and others, 1980). Akutan Island samples plot along the same trend as volcanics and intrusions from Unalaska Island but tend to be lower in Sr. Appendix E lists the results of Rb and Sr analyses.

Figures 27 and 28 are plots of Rb versus Rb/Sr and Sr versus Rb/Sr, respectively. These two diagrams successfully distinguish Lava Peak volcanics (higher Sr and lower Rb and Rb/Sr) from the other volcanics on the island.

McCulloch and Perfit's (1981) data are also plotted on the two diagrams. Two samples, AK-4-EJ and -33, plot in the Lava Peak field but the third sample does not show a close relationship to either group. Unfortunately, it is not known whether the petrology of his samples is similar to that of the Lava Peak flows.

McCulloch and Perfit (1981) distinguished tholeiitic Akutan rocks from calc-alkaline rocks in the Aleutians by plotting Ba (ppm) versus K_2O and Rb/Sr versus K_2O. Their results suggest that tholeiitic rocks have higher Ba and Rb/Sr values for a given K_2O than the calcalkaline suites. Akutan samples plot in McCulloch and Perfit's tholeiitic region for K_2O versus Rb/Sr, but the separation between the tholeiitic and cal-alkaline fields is not very good and the fields overlap at the mafic end.

McCulloch and Perfit's (1981) Sr and Nd isotope data for Akutan are shown in table 7 and are comparable to results reported by other workers (Kay and others, 1978; Kay, 1980; Marsh, 1976) for Aleutian lavas.

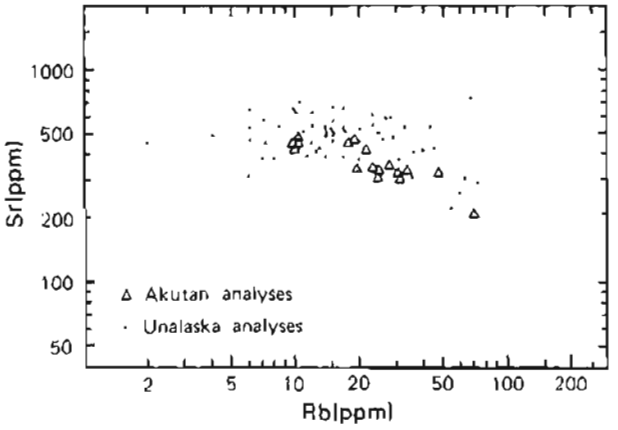

Figure 26. *Sr versus Rb diagram. Unalaska analyses taken from Perfit and others (1980).*

Table 7. *Neodymium and strontium data for Akutan Island*

Location	Sample	$^{87}Sr/^{86}Sr$	$^{143}Nd/^{144}Nd$
SE of Akutan Harbor	AK4-EJ	0.70342±44	0.51219±3
Akutan Harbor	AK4-3	0.70315±5	–
Hot Springs Bay Valley	AK4-15	0.70317±4	0.51225±2
Akutan Harbor	AK4-22	0.70302±6	–
Sarana Bay	AK4-33	0.70308±5	0.51220±2
Sarana Bay	AK4-47	0.70324±3	–

Data from McCulloch and Perfit (1981) and Perfit (unpublished data). Errors are in the last figures given and represent ±2 mean.

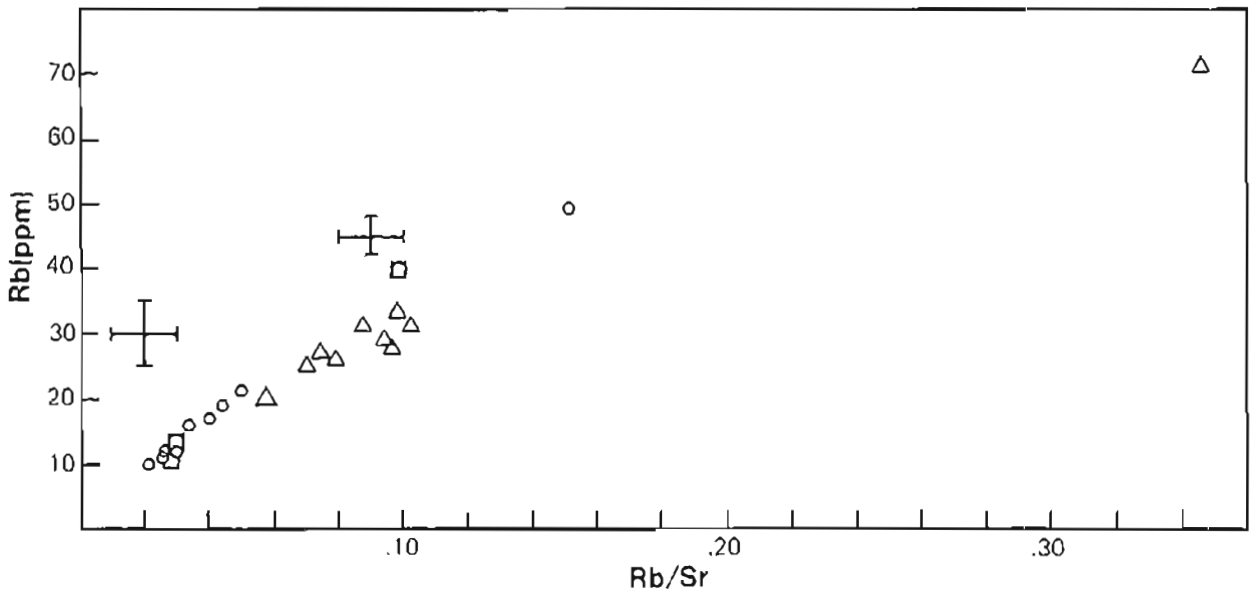

Figure 27. *Rb versus Rb-Sr diagram. Crosses indicate typical precision. Circle = Lava Peak rocks; triangles = lavas from elsewhere on the island; squares = samples from Perfit and others (1980).*

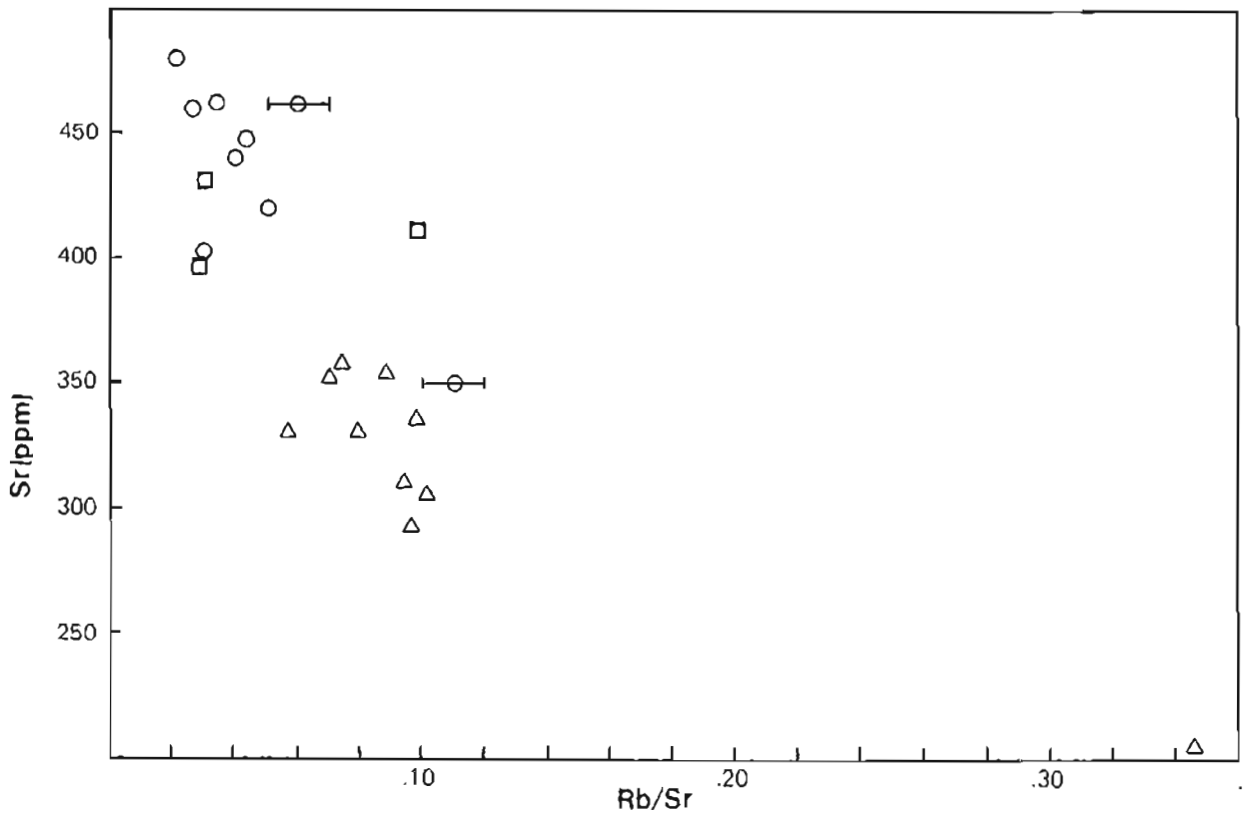

Figure 28. *Sr versus Rb-Sr diagram. Bar indicated typical precision. Open circle = Lava Peak rocks; triangles = lands from elsewhere on the island; square = samples from Perfit and others (1981).*

POTASSIUM-ARGON DATES

Four K-Ar whole rock dates were obtained from R. Armstrong at the University of British Columbia, Vancouver, for two samples from eastern Akutan and two from Lava Peak (table 8). Lava flows from Lava Peak, Pickup Valley, and Hot Springs Bay Valley give ages around 1.2 Ma. AK-81-30, a dike from the base of Lava Peak, may be about 0.3 Ma older than the three flows dated.

Both oxide-oxide plots and multivariate statistical analyses indicate that the major element chemistry of two petrographic groups of lava follow similar trends. Rb and Sr plots successfully distinguish the two petrographic groups and suggest that the two groups may be related via some fractionation scheme. This is also indicated by the decrease in CaO/Al_2O_3 with increasing FeO*/MgO (fig. 22). Whole-rock potassium-argon dates indicate that the Lava Peak satellite vent and the main-vent lava suites erupted contemporaneously between 1.1 and 1.5 Ma. The major-element chemistry of these lavas is typical of rocks derived from mantle material (McCulloch and Perfit, 1981). Neodymium and strontium isotope ratios reported by McCulloch and Perfit (1981) also suggest that the lava were derived from mantle material and that contamination by continental crust was negligable.

Table 8. *Whole-rock K-Ar dates for Akutan lavas*

[Analytical work for this study done under the direction of R. Armstrong, University of British Columbia, Vancouver, Canada. LP - Lava Peak, PV - Pickup Valley, HSBV - Hot Springs Bay Valley, L - lower series, F - lava flows, rAr^{40} - radiogenic argon.]

Location	Sample	K (wt%)	rAr^{40} 10^{-10}mole/g	rAr^{40} (%)	Date ($x10^6$ yr)
LP(L)	AK-81-14	0.691	0.0133	8.5	1.1 ± 0.2
LP(L)	AK-81-30	0.648	0.0175	23.8	1.5 ± 0.1
PV(F)	AK-81-23	1.23	0.0305	10.0	1.4 ± 0.2
HSBV	AK-80-9a	0.806	0.0159	13.6	1.1 ± 0.1

GEOTHERMOMETRY AND GEOBAROMETRY

Two geothermometers and one geobarometer were used to estimate equilibrium temperatures and pressures for mineral pairs in Akutan lavas. Both geothermometers could not be used on the same samples because none of the samples analyzed by microprobe contained the three phases needed.

Wood and Banno's (1973) geothermometer used the distribution of FeO and MgO between orthopyroxene and clinopyroxene to determine the equilibrium temperature. This geothermometer was used on a sample collected from Pickup Valley (AK-81-23). Wells (1977) modified Wood and Banno's geothermometer by using additional microprobe data. His geothermometer is used to corroborate the results obtained from Wood and Banno's (1973) geothermometer. Powell and Powell's (1974) geothermometer used the distribution of Mg and Fe between olivine and clinopyroxene to determine equilibrium temperatures. This geothermometer was used on two samples from Lava Peak (AK-81-1 and -13). The results for the geothermometry are shown in table 6. They indicate equilibrium temperatures between 992 °C and 1,180 °C for both sets of mineral pairs.

Wood (1976) noted several problems with the olivine-clinopyroxene geothermometer that would result in temperature estimates that did not reflect the actual crystallization temperature but seem geologically reasonable. The temperature-determining equation for Powell and Powell's (1974) geothermometer is:

$$T = \frac{-2X_{Al}\,(920000+3.6P)-0.0435\,(P-1)+10100}{8 + R\ln D - 714.3\,(2X_{Al})}$$

where

$$X_{Al} = X_{Al} + X_{Ti} + X_{Cr} + X_{Fe}$$

$$D = \left(\frac{X_{Mg,ol}}{X_{Fe,ol}}\right)\left(\frac{X_{Fe,M1}}{X_{Mg,M1}}\right)$$

$X_{Fe,ol}$ and $X_{Mg,ol}$ equal the mole fractions of Fe and Mg in olivine, respectively, and M1 is a specific octahedral site in clinopyroxene.

$$X_{Fe,M1} = \frac{H1}{1+\left(\frac{X_{Mg}}{X_{Fe}}\right)_{cpx}}$$

$$X_{Mg,M1} = H1 - X_{Fe,M1}$$

$H1 = 1\text{-}X_{Al}$
R = 1.98726 cal/mole K
P = pressure in bars
ol = olivine, cpx = clinopyroxene, opx = orthopyroxene

Other difficulties involve the pressure dependence of the olivine-clinopyroxene geothermometer and whether the phenocrysts used are in equilibrium. A crystallization pressure must be supplied in the equation to determine the temperature. The values listed in table 6 are for pressures between 1 bar and 15 kb.

The olivine in Akutan lavas commonly occurs as both skeletal and subhedral grains. Both types of phenocrysts are similar in composition. This may be due to buffering of the olivine composition by the liquid or to the two types of grains crystallizing during the same period. If both types of grains crystallized during the same interval, the skeletal olivine indicates crystallization at higher undercooling temperatures. The clinopyroxene is subhedral, suggesting that it crystallized at a lower undercooling than the skeletal olivine. Clinopyroxene crystals are zoned over a compositional range of 5 mole-percent, whereas zoning of both phenocrysts may mean they formed under similar conditions and are in equilibrium with each other.

Wood and Banno (1973) felt that pressure effects on their geothermometry could be ignored. This presumption was based upon experimental evidence published by Davis and Boyd (1966) which indicated only a 50 °C change in the calculated temperature with a 30 kb change in pressure. This was within the error of the technique. Wood and Banno (1973) also assumed that any Al_2O_3 in the pyroxenes would not appreciably affect the activity of Mg in either of the pyroxenes.

The determining equation is:

$$T = \frac{-10202}{\ln\left(\frac{A_{Mg}^{cpx}}{A_{Mg}^{opx}}\right) - 7.65X_{Fo}^{opx} + 3.88\left(X_{Fe}^{opx}\right)^2 - 4.6}$$

where

$$A_{Mg}^{cpx,opx} = \left(\frac{Mg^{2+}}{Fe+Mg^{2+}+Ca^{2+}+Mn^{2+}+Na^{+}}\right)_{M2} \bullet \left(\frac{Mg^{2+}}{Fe^{2+}+Fe^{3+}+Mg^{2+}+Al^{3+}+Cr^{3+}+Ti^{4+}}\right)_{M1}$$

X_{Fe}^{opx} = mole-percent Fe in orthopyroxene and
M1, M2 are specific octahedral sites in clinopyroxene

All amounts are in mole fractions. Wood and Banno (1973) feel that the temperatures are accurate to ± 70 °C. They ignore Fe^3 in the pyroxenes because if 10 percent of the Fe^2 is Fe^3, the equilibrium temperature goes up 20 °C to 30 °C, which is within the error of the technique.

Wells (1977) modified Wood and Banno's (1973) pyroxene geothermometer to fit additional pyroxene equilibrium data. Wells' corrections may alter the temperature estimate.

The determining equation is:

$$T = \frac{7341}{3.355+244X_{Fe}^{opx} - \ln K}$$

where K= the activity of Mg in clinopyroxene
divided by the activity of Mg in orthopyroxene
(see Wood and Banno, 1973)

where X_{Fe}^{opx} = mole-percent Fe in orthopyroxene

The temperatures obtained form this geothermometer are listed in table 6.

The lack of precision in these temperature estimates results from the insufficient data available regarding the thermodynamics that govern Fe and Mg substitution in cation sites. These temperatures should be considered rough estimates of equilibrium temperature for the mineral pairs concerned, not accurate measurements.

As yet, no good geobarometers have been developed for mafic igneous rocks. Finnerty (1976) examined the exchange of Mn, Ca, Mg, and Al between garnet, olivine, clinopyroxene, and orthopyroxene in an attempt to develop a suitable geothermometer and geobarometer. To use their geobarometer, olivine must be in equilibrium with orthopyroxene and clinopyroxene because the pyroxene pair buffered the system with respect to calcium. Finnerty and Boyd (1977) worked with ultramafic rocks and the two pyroxenes were the only calcium-bearing phases present. None of the rocks examined in this study contain all three mafic minerals, but plagioclase is always present and may act as a calcium buffer for the system. If it is valid to use plagioclase as a buffer, Finnerty and Boyd's technique suggests that the olivine crystallized at some pressure less than 10 kb, which is consistent with the experimental studies of Baker and Eggler (1983).

From the crystallization sequence of phases in Aleutian lavas, Marsh (1976) estimated their crystallization temperatures to be between 1,150 °C and 1,101 °C, at pressures between 1 and 5 kb. Perfit and Gust's (1981) estimate of crystallization temperatures based on orthoclinopyroxene pairs ranges between 990 °C and 1,100 °C. These values compare well with those discussed above. Marsh (1976) noted that other workers found that plagioclase was the liquidus phase in andesitic magmas with less than 2 percent water (Eggler and Burnham, 1973). For water-saturated conditions, plagioclase was replaced by orthopyroxene as the liquidus phase above about 500 bars pressure. Marsh concluded that crystallization took place at about 500 bars in andesitic magmas with less than 2 percent water.

The temperatures obtained from the geothermometers are in the range expected for an erupting magma but do not provide any additional information regarding the origin of Akutan lavas.

MAGMA GENERATION MODELS

Several models have been suggested to account for the chemical composition of Aleutian lavas. Most of these involve partial melting of oceanic crust with some oceanic sediments or depleted mantle or combinations thereof to account for the minor-element and rare-earth-element (REE) abundances.

Coats (1962) used a "megathrust" to carry sediments down to mantle depths, where they melted to form a rhyolitic melt. The melt then mixed with basaltic liquids to form andesitic magmas. Marsh (1976) derived Aleutian magmas from partial melts of subducted oceanic crust. He argued that there was not enough water in the mantle to form the magmas, and a more likely place would be subducted oceanic crust. Marsh did not use sediment contamination to modify the magma.

McCulloch and Perfit (1981) argued that REE and minor-element ratios precluded the formation of Aleutian magmas directly from melted oceanic crust. Rather, a multistage mixing-melting model was invoked in which the depleted mantle below the arc is metasomatized by a partial melt of oceanic crust. McCulloch and Perfit suggested that between 2 and 8 percent oceanic sediments are required to generate the variable large-ion lithophile enrichments and Sr and Nd isotope values in these magmas.

Kay and others (1978) also argued for sediment mixing to account for Pb and Sr values differing from those of Mid Ocean Ridge Basalts (MORB). Aleutian samples have Pb isotope ratios between those of MORB and Pacific sediments, which can be accounted for by contamination of about 2 percent sediments. Both Kay and others (1978) and McCulloch

and Perfit (1981) note that the lack of variability and low values of the Sr isotope ratios indicate that passage through old continental material has not affected the composition of these magmas.

Perfit and Gust (1981) suggested that the high-magnesium basalts found on Akutan and Unalaska islands could represent primary magmas. The high-alumina basalts and basaltic andesites seen on the islands could be generated by fractionation of olivine, clinopyroxene, and plagioclase from the magnesium-rich basalts. Kay (1978) also suggested that these high-magnesium lavas were primary melts.

Eichelberger (1978) derived andesites from a mixture of rhyolite and depleted mantle. He suggested that under hydrous conditions, the lower oceanic crust would be amphibolite. Up to a 20-percent melt derived from this composition would be rhyolitic. This rhyolitic component would mix with a basaltic melt derived from mantle material to form andesites.

Kay (1980) modeled magma generation by using mass-balance calculations and concluded that the variety of magma types in the Aleutians are due to partially melting different amounts of subducted sediments, oceanic crust, and depleted mantle.

The diversity of opinion regarding the origin of andesitic magma indicates the lack of knowledge of both mantle composition and the role played by the subducted oceanic slab and sediments. It is agreed that magmas are related to regions of subduction, but the role of the subducted slab, mantle, and sediments in the development of andesitic magmas is still under debate.

EVOLUTION OF IGNEOUS ROCKS ON NORTHERN AKUTAN ISLAND

The lack of continuous outcrop makes it difficult to ascribe any detailed petrologic trends to Akutan lavas. The only location on northern Akutan Island where flows are exposed in a section not separated by debris flow deposits is at Lava Peak. There, the lower series of lava flows follows a typical trend for a fractionating magma: the lavas become more silica-rich upsection, and the percentage of mafic minerals decreases with increasing silica content. Elsewhere on the island, exposures do not allow for similar interpretations. Flows are commonly separated by thick sequences of pyroclastic debris, making it impossible to determine whether a sequence of flows is the product of one magma, or more than one.

Two petrographic groups are present on Akutan Island: Lava Peak flows and dikes, and lavas exposed elsewhere on the island. Clinopyroxene and orthopyroxene are the major mafic minerals in the latter lavas, whereas olivine and clinopyroxene are the mafic minerals in Lava Peak flows. Only rarely is olivine present in other lavas from Akutan Island, and even more rarely is it abundant. This appears to be due to higher silica values, making orthopyroxene the stable mafic phase. The most recent volcanics, the pre-1870 and 1978 lava flows, are petrologically similar to volcanics exposed on the central and eastern part of the island (table 4).

Many aspects of the major-element chemistry of the two petrologic groups are quite similar. Oxide diagrams and multivariate statistical analyses do not suggest any differences either in the way the two groups fractionated or their parental magmas. The use of TiO_2 and P_2O_5 as discriminates indicates that the variance of the more abundant oxides is too great to be able to distinguish the four groups identified by the cluster analysis. Even these two oxides cannot clearly distinguish between the two groups of lava flows, although they are able to distinguish between flows and dikes.

Both the Rb and Sr analyses and the plagioclase microprobe analyses suggest compositional differences between Lava Peak flows and other lavas on the island. The Lava Peak flows are higher in Sr and lower in Rb and Rb/Sr than lavas from the rest of the island. Lava Peak flows appear to have a more calcic plagioclase than plagioclase in lavas from other parts of the island.

Whole-rock potassium-argon dates of three lava flows and one dike indicate volcanic activity began at least 1.5 Ma. The Lava Peak flows and lava flows from the eastern and central part of the island were erupting contemporaneously about 1.1 Ma.

Any model developed to explain the igneous activity on Akutan Island must explain: (1) the different mineral assemblages, (2) the overall chemical similarity between the two petrographic groups, (3) the differences in Rb and Sr contents, (4) the differences in phenocryst abundance, and (5) the identical radiometric ages of the two groups of flows.

One model that accounts for these differences relies on a compositionally zoned magma chamber (fig. 29). According to this model, the lavas exposed over most of the island are from central-vent eruptions, which drew magma from the top of the chamber. Lava Peak flows are from lateral eruptions, which tapped magma lower in the chamber. Crystallization and settling of early-forming plagioclase, olivine, and clinopyroxene from the upper part of the magma chamber would create an upper layer deficient in phenocrysts and enriched in silica and incompatable elements. The local concentration of these phenocrysts would create a lower layer enriched in phenocrysts and relatively silica deficient. Lavas erupting from the top of the magma chamber would be relatively phenocryst poor and sufficiently enriched in silica that orthopyroxene would replace olivine as the first mafic phase to crystallize, resulting in fine-grained rocks containing orthopyroxene and clinopyroxene phenocrysts.

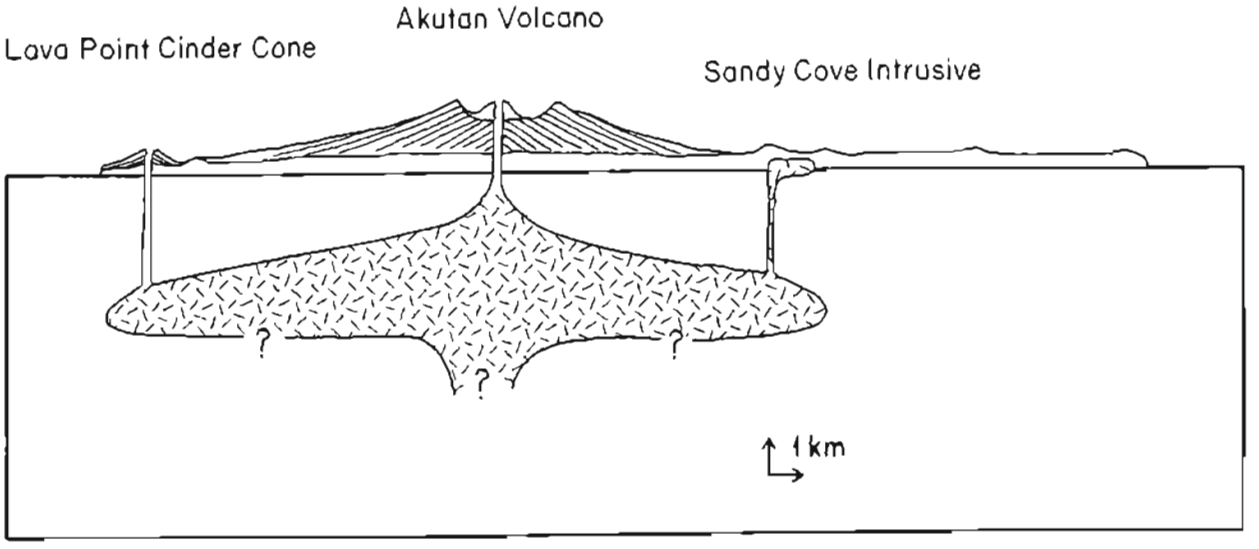

Figure 29. *Sketch of Akutan Island showing the central vent, Lava Peak, and zoned magma chamber.*

The Lava Peak eruptions, tapping a lower layer in the chamber, would be enriched in early-formed phenocrysts and relatively silica poor. The result would be phenocryst-rich rocks containing olivine and clinopyroxene. The tholeiitic character of Akutan lavas is the result of iron enrichment in the liquid caused by the suppression of iron-oxide precipitation.

Different Rb and Sr abundances in the two petrologic groups result from partitioning of the two cations in the melt. Rb (eightfold coordination) cations have ionic radii of 1.49A, whereas (sixfold to eightfold coordination) cations have ionic radii of 1.16A (Shannon and Prewitt, 1969). The smaller divalent Sr cation can substitute for Ca (ionic radius = 1.00A) in plagioclase, whereas Rb is excluded from the plagioclase crystal lattice and is concentrated in the residual liquid. The early-forming plagioclase would selectively remove Sr from the upper layer of the magma chamber, leaving a liquid relatively enriched in Rb. The lower layer, enriched in plagioclase phenocrysts, would also be enriched in Sr. Magma drawn from the upper layer would have more Rb and less Sr than magma from lower layers.

The overall chemical similarity between the two petrologic groups is due to their derivation from the same magma body; however, some magma mixing may have complicated many of the simple trends seen. Simultaneous eruptions from different regions of the magma chamber resulted in lavas with the same radiometric age but different characteristics.

Magma composition on Akutan Island has not changed appreciably through time. While Lava Peak flows can be distinguished from the other lava flows on the island, the small range in chemical composition for these lavas makes evolutionary interpretation impossible. This compositional monotony is characteristic of Aleutian lavas and suggests that the magmas erupt so quickly that they do not differentiate significantly or are replenished by the source material, resulting in lavas of relatively uniform composition.

Dike orientations on Lava Peak, the location of the Lava Peak center, and the location of the recent cinder cone and lava flow suggest a persistent zone of weakness existing on the northwestern side of the island since at least 1.5 Ma.

The character of rocks from this zone has changed such that the most recent lavas are similar to the main-vent lavas, not the Lava Peak flows.

Akutan Island is composed of basaltic and andesitic lavas, ranging from 46 to 63 percent silica; compositions typical of other Aleutian volcanoes (Byers, 1959; Drewes and others, 1961; Marsh, 1976; Kay and others, 1982). Mineral compositions are also similar between various volcanoes (Byers, 1959; Drewes and others, 1961; Marsh, 1976; Perfit and Gust, 1981). The similarity in oxide analyses, mineralogy, and isotopic ratios suggests that both Akutan lavas and the other Aleutian volcanoes are derived from a similar-if not the same-source.

Current theories suggest that Aleutian magmas result from partially melted oceanic crust or mantle, contaminated by 2 to 8 percent sediments, which rises through the overlying plate and erupts on the surface. Nd and Sr isotope analyses indicate a mantle origin for Akutan lavas (McCulloch and Perfit, 1981; DePaolo, 1981). Ba/La and Pb/La ratios suggest that continental sediments also play a role in the development of Akutan magmas.

Volcano distribution in island arcs may be due to segmentation of the subducting oceanic plate (Stoiber and Carr, 1973; Hughes and others, 1980). Kay and others (1982) developed a segmentation model to explain the distribution of tholeiitic and calc-alkaline volcanoes in the Aleutian arc. Kay and others' (1982) model restricts tholeiitic volcanoes to segment boundaries, whereas calc-alkaline volcanoes are found only in segment interiors. They argue that these two types of volcanoes reflect different stress regimes in the Aleutian crust. Tholeiitic volcanoes form in areas of relative extension whereas calc-alkaline volcanoes form in areas of compression. The segment boundaries are delineated by zones of great earthquake movements, and tectonic features on the North American and subducting Pacific plates. Akutan Island is in the middle of their Cold Bay segment. According to their model, Akutan lavas should be calc-alkaline; instead they show tholeiitic affinities (Perfit and Gust, 1981). Kay and others' model breaks down because little petrologic information is available for volcanoes in the eastern Aleutian arc. Whether tholeiitic and calc-alkaline volcanoes fit into a segmentation model will not be clear until much more information is gathered on the petrology and geochemistry of the region.

This study describes the petrology and geochemistry on northern Akutan Island. The southern half of the island should be examined in similar detail. In particular, Flat Tip Peak should be examined to see if it is petrologically similar to Lava Peak. Additional plagioclase microprobe analyses should be conducted to see if the compositional difference between Lava Peak plagioclase and the other lavas is a phenomenon. More potassium-argon dates are needed to define the period of igneous activity. It is not known what compositional type (tholeiitic or calc-alkaline) is currently erupting from Akutan Volcano. A detailed study of the geochemistry and petrology of the volcano is needed to identify the current trend and describe its relation to other lavas.

REFERENCES

Baker, D.R., and Eggler, D.H., 1983, Fractionation paths of Atka (Aleutians) high-alumina basalts; constraints from phase relations: Journal of Volcanology and Geothermal Research, v. 18, p. 387-404.

Bhattacharji, S., and Smith, C.H., 1964, Flow differentiation: Science, v. 145, p. 150-153.

Black, R.F., 1974, Geology and ancient Aleuts, Amchitka and Umnak Island, Aleutians: Arctic Anthropology, XI-2, p. 126-140.

Byers, F.M., Jr., 1959, Geology of Umnak and Bogoslof Islands, Aleutian Islands, Alaska: U.S. Geological Survey Bulletin 1028-L, p. 267-352.

Byers, F.M., Jr., and Barth, T.F.W., 1953, Volcanic activity on Akun and Akutan Islands: Pacific Science Conference, 7th, New Zealand, 1949, Proceedings, v. 2, p. 382-397.

Coats, R.R., 1962, Magma type and crustal structure in the Aleutian arc, *in* McDonald, G.A., and Kuno, Hisashi, eds., The crust of the Pacific basin: American Geophysical Union: Geophysical monograph 6, p. 92-109.

Cox, K.G., Bell, J.D., and Pankhurst, R.J., 1979, The interpretation of igneous rocks: London, George Allen and Unwin, 450 p.

Davis, B., and Boyd, F., 1966, The join $Mg_2Si_2O_6$--$CaMgSi_2O_6$ at 30 kilobars pressure and its application to pyroxenes from kimberlites: Journal of Geophysical Research; v. 71, p. 3567-3576.

Davis, J.C., 1973, Statistics and data analysis in geology: New York, John Wiley & Sons, 550 p.

Deer, W.A., Howie, R.A., and Zussman, J., 1978, Rock-forming minerals: Single Chain Silicates: New York, John Wiley and Sons, v. 2A, 668 p.

DePaolo, D.J., 1981, Nd isotope studies: some new perspectives on earth structure and evolution: EOS, v. 62, no. 14, p. 137-140.

Drewes, H., Fraser, G.D., Snyder, G.L., and Barnett, H.F., 1961, Geology of Unalaska Island and adjacent insular shelf, Aleutian Island, Alaska: U.S. Geological Survey Bulletin 1028-S, p. 583-676.

Eggler, D.H., and Burnham, C.W., 1973, Crystallization and fractionation trends in the system andesite-H_2O-CO_2-O_2 at pressures to 10 kb: Geological Society of America Bulletin, v. 84, p. 2517-2532.

Eichelberger, J.C., 1978, Andesitic volcanism and crustal evolution: Nature, v. 275, p. 21-27.

Finch, R.H., 1935, Akutan Volcano: Zeitschrift für Vulkanologie; Band XVI, p. 155-160.

Finnerty, A.A., 1976, Exchange of Mn, Ca, Mg, and Al between synthetic garnet, orthopyroxene, and olivine: Washington, D.C., Carnegie Institution Geophysical Laboratory 1976 Yearbook, p. 572-579.

Finnerty, A.A., and Boyd, F.R., 1977, Pressure-dependent solubility of calcium in forsterite coexisting with diopside and enstatite: Washington, D.C., Carnegie Institution Geophysical Laboratory 1977 Yearbook, p. 713-717.

Gibb, F.G., 1972, Flow differentiation in the xenolithic ultrabasic dykes of the Cuillins and the Strathaird Peninsula, Isle of Skye, Scotland: Journal of Petrology, v. 9, p. 411-443.

Gray, N.H., 1971, A parabolic hourglass structure in titanaugite: The American Mineralogist, v. 56, p. 952-958.

Hollister, L.S., and Gancarz, A.J., 1971, Compositional sector-zoning in clinopyroxene from Narce area, Italy: The American Mineralogist, v. 56, p. 959-979.

Hughes, H.M., Stoiber, R.E., and Carr, M.J., 1980, Segmentation of the Cascade volcanic chain: Geology, v. 8, p. 15-17.

Jennrich, R.I., 1977, Stepwise discriminant analysis, *In* Enslein, K., Ralston, A., and Wilf, H., eds., Statistical methods for digital computers: New York, Wiley-Interscience, v. III, p. 76-95.

Jennrich, R.I., and Sampson, P., 1981, Stepwise discriminant analysis, *In* Dixon, W.J., ed., BMDP statistical software: Berkeley, University of California Press, p. 519-537.

Kay, R.W., 1978, Aleutian magnesium andesites: Melts from subducted Pacific Ocean crust: Journal of Volcanology and Geothermal Research, v. 32, no. 4, p. 117-132.

_____1980, Volcanic arc magmas: Implications of a melting-mixing model for element recycling in the crust-upper mantle system: Journal of Geology, v. 88, no. 5, p. 497-522.

Kay, R.W., Sun, S.S., and Lee-Hu, C.N., 1978, Pb and Sr isotopes in volcanic rocks from the Aleutian Islands and Pribilof Islands, Alaska: Geochemica et Cosmochimica Acta, v. 42, p. 263-273.

Kay, S.M., Kay, R.W., and Citron, G.P., 1982, Tectonic controls on tholeiitic and calc-alkaline magmatism in the Aleutian arc: Journal of Geophysical Research, v. 87, p. 4051-4072.

Komar, P.D., 1972a, Mechanical interactions of phenocrysts and flow differentiation of igneous dikes and sills: Geological Society of America Bulletin, v. 83, p. 973-987.

_____1972b, Flow differentiation of igneous dikes and sills; profiles of velocity and phenocryst concentration: Geological Society of America Bulletin, v. 83, p. 3443-3448.

Kuno, Hisashi, 1966, Lateral variation of basalt magma type across continental margins and island arcs: Bulletin Volcanologique, v. 29, p. 195-222.

Lofgren, G., 1980, Experimental studies on the dynamic crystallization of silicate melts, *in* Hargraves, R.B., ed., Physics of magmatic processes: Princeton, N.J., Princeton University Press, p. 487-551.

Maaloe, Sven, and Peterson, T.S., 1981, Petrogenesis of oceanic andesites: Journal of Geophysical Research, v. 86, p. 10273-10286.

Marsh, B.D., 1976, Some Aleutian andesites: their nature and source: Journal of Geology, v. 84, no. 1, p. 27-46.

_____1979, Island-arc development: some observations, experiments, and speculation: Journal of Geology, v. 87, p. 687-713.

McCulloch, M., and Perfit, Michael, 1981, $^{143}Nd/^{144}Nd$, $^{87}Sr/^{86}Sr$ and trace-element constraints on the petogenesis of Aleutian island-arc magmas: Earth and Planetary Science Letters, v. 56, p. 167-179.

McCammon, R.B., and Wenniger, G., 1970, The dendrograph: Kansas State Geological Survey: Computer Contribution 48.

Miyashiro, H., 1974, Volcanic rock series in island arcs and active continental margins: American Journal of Science, v. 274, no. 4, p. 321-355.

Morgan, L.W., ed., 1980, The Aleutians: Alaska Geographic, v. 7, no. 3, p. 224.

Mottl, M.J., and Holland, H.D., 1978, Chemical exchange during hydrothermal alteration of basalt by seawater - I. Expermental results for major and minor components of seawater: Geochimica et Cosmochimica Acta, v. 42, p. 1103-1115.

Motyka, R.J., Moorman, M.A., and Liss, S.A., 1981, Assessment of thermal springs sites, Aleutian arc, Atka Island to Becherof Lake--preliminary results and evaluation: Alaska Division of Geological and Geophysical Surveys Open-file Report 144, p. 90-96.

Motyka, R.J., Wescott, E.M., Turner, D.L., Swanson, S.E., Allely, R.D., and Larsen, Mark, 1988, Introduction and summary of geothermal investigations in Hot Springs Bay Valley, Akutan Island, Alaska, *in* Motyka, R.J. and Nye, C.J., eds., A geological, geochemical, and geophysical survey of the geothermal resources at Hot Springs Bay Valley, Akutan Island, Alaska: Alaska Division of Geological and Geophysical Surveys Report of Investigations 88-3, p. 1-10.

Perfit, Michael, 1978, The petrochemistry and strontium isotope composition of mafic basalts from the Aleutian Islands [abs.]: Annual Meeting of Geological Society of America, p. 470.

Perfit, Michael, Brueckner, H., Lawrence, J., and Kay, R.W., 1980, Trace-element and isotopic variation in a zoned pluton and associated rocks, Unalaska Island, Alaska: A model for fractionation in the Aleutian calcalkaline suite: Contributions to Mineralogy and Petrology, v. 73, p. 69-87.

Perfit, Michael, and Gust, D., 1981, Petrochemistry and experimental crystallization of basalts from the Aleutian Islands, Alaska [abs.]: IAVCEI Symposium on Arc Volcanism, p. 288-289.

Powell, Marjorie, and Powell, Roger, 1974, An olivine-clinopyroxene geothermometer: Contributions to Mineralogy and Petrology, v. 48, p. 249-263.

Shannon, R.D., and Prewitt, C.T., 1969, Effective ionic radii in oxides and fluorides: Acta Crystallographica, p. 925-946.

Simkin, T., Siebert, L., McCelland, L., Bridge, D., Newhall, C., and Latter, J., 1981, Volcanoes of the World: The Smithsonian Institution, Stroudsburg, Pennsylvania, Hutchison Ross Publishing Company, p. 232.

Stewart, D.C., 1975, Crystal clots in calc-alkaline andesites as breakdown products of high-Al amphiboles: Contributions to Mineralogy and Petrology, v. 53, p. 195-204.

Stoiber, R.E., and Carr, M.J., 1973, Quaternary volcanic and tectonic segmentation of Central America: Bulletin Volcanologique, v. 37, p. 304-325.

Strong, D.F., 1969, Formation of the hour-glass structure in augite: Mineralogical Magazine, v. 37, no. 288, p. 472-479.

Swanson, S.E., and Romick, J.D., 1988, Geology of northern Akutan Island, *in* Motyka, R.J. and Nye, C.J., eds., A geological, geochemical, and geophysical survey of the geothermal resources at Hot Springs Bay Valley, Akutan Island, Alaska: Alaska Division of Geological and Geophysical Surveys Report of Investigations 88-3, p. 11-27.

Wass, S.Y., 1973, The origin and petrogenetic significance of hour-glass zoning in titaniferous clinopyroxenes: Mineralogical Magazine, v. 39, no. 302, p. 133-144.

Wells, P.R.A., 1977, Pyroxene thermometry in simple and complex systems: Contributions to Mineralogy and Petrology, v. 62, p. 129-139.

Wood, B.J., 1976, An olivine-clinopyroxene geothermometer: Contributions to Mineralogy and Petrology, v. 56, p. 297-303.

Wood, B.J., and Banno, S., 1973, Garnet-orthopyroxene and orthopyroxene-clinopyroxene relationships in simple and complex systems: Contributions to Mineralogy and Petrology, v. 42, p. 109-124.

APPENDIX A
Petrographic Descriptions of Akutan Lavas

Sample	Description
AK-81-22	Porphyritic andesite containing about 8 percent phenocrysts (plagioclase, orthopyroxene, and clinopyroxene).
AK-81-1	Porphyritic basalt dike containing plagioclase, clinopyroxene, and olivine phenocrysts in a holocrystalline groundmass.
AK-81-2	Porphritic basalt lava flow containing olivine, clinopyroxene, and plagioclase phenocrysts in a holocrystalline groundmass.
AK-81-3	Pophyritic basalt lava flow containing the same mineralogy as AK-81-2.
AK-81-4	Similar mineralogy and texture to AK-81-2.
AK-81-5	Similar to AK-81-2.
AK-81-6	Similar to AK-81-2.
AK-81-7	Similar to AK-81-2.
AK-81-8	Similar to AK-81-2.
AK-81-9	Similar to AK-81-2.
AK-81-10	Similar to AK-81-2.
AK-81-11	Similar to AK-81-2.
AK-81-12	Similar to AK-81-2.
AK-81-13	Similar to AK-81-2.
AK-81-14	Similar to AK-81-2.
AK-81-16	Porphyritic andesite lava flow containing plagioclase, olivine, and clinopyroxene phenocrysts in a very fine grained, vesicular groundmass.
AK-81-17	Prophyritic andesite lava flow containing plagioclase, clinopyroxene, orthopyroxene, and trace olivine phenocrysts in a very fine grained groundmass.
AK-81-18	Prophyritic andesite lava flow containing plagioclase, olivine, clinopyroxene, and orthopyroxene phenocrysts in a fine-grained groundmass.
AK-81-19	Float from the northern flank of Akutan Volcano. Porphyritic rock containing plagioclase, olivine, orthopyroxene, and clinopyroxene phenocrysts in a vesicular glassy groundmass.
AK-81-20	Andesite from Pickup Valley. Porphyritic rock containing plagioclase, orthopyroxene, and clinopyroxene phenocrysts in a trachytic groundmass.
AK-81-21	Andesite plug containing clinopyroxene and plagioclase phenocrysts. The groundmass is partially altered to chlorite and carbonate. Quartz veinlets intrude the rock.

APPENDIX A *(continued)*

Sample	Description
AK-81-22	Porphyritic andesite containing about 8 percent phenocrysts (plagioclase, orthopyroxene, and clinopyroxene).
AK-81-23	Porphyritic, partially altered andesite lava flow. The rock contains clinopyroxene, orthopyroxene, and plagioclase phenocrysts in a trachytic groundmass that is partially altered to carbonate.
AK-81-24	Porphyritic andesite lava flow containing phenocrysts of plagioclase, clinopyroxene, and olivine in a trachytic groundmass. The olivine is largely altered to serpentine minerals, whereas the clinopyroxene and groundmass are partially altered to carbonate and chlorite.
AK-81-26	Aphanitic basalt flow. Trace plagioclase phenocrysts in a very fine grained trachytic groundmass consisting of olivine, clinopyroxene, opaques, and plagioclase.
AK-81-27	Porphyritic andesite lava flow containing clinopyroxene, orthopyroxene, plagioclase, and trace olivine phenocrysts in a brown, vesicular, glassy groundmass.
AK-81-28	Similar mineralogy and texture to AK-81-27.
AK-81-29	Similar mineralogy and texture to AK-81-27.
AK-81-30	Aphanitic basaltic dike consisting of an equigranular mass of olivine, clinopyroxene, plagioclase, and opaque minerals.
AK-81-31	Porphyritic andesite dike containing plagioclase phenocrysts in a fine-grained vesicular groundmass consisting of olivine, plagioclase, clinopyroxene, and opaque minerals.
AK-81-32	Aphanitic dike. Contains rare plagioclase phenocrysts in a very fine grained vesicular groundmass.
AK-81-33	Similar to AK-81-32. The groundmass has a trachytic texture and contains brown glass.
AK-81-34	Slightly porphyritic dike containing large plagioclase and clinopyroxene phenocrysts in a fine-grained groundmass.
AK-81-35	Porphyritic andesite lava flow containing plagioclase, clinopyroxene, and rare olivine phenocrysts in a glassy trachytic groundmass.
AK-81-36	Altered andesite dike. Plagioclase phenocrysts in a partially altered, fine-grained groundmass. The mafic phenocrysts have been altered to chlorite and carbonate.
AK-81-37	Altered andesite dike. Two percent plagioclase phenocrysts in an altered groundmass.
AK-81-38	Partially altered porphyritic andesite dike. The rock contains plagioclase, clinopyroxene, and opaque phenocrysts in a fine-grained trachytic groundmass. The phenocrysts are usually in the form of crystal clots.
AK-81-40	Partially altered porphyritic andesite dike. The rock contains plagioclase phenocrysts in a dark-brown groundmass. The mafic phenocrysts have been altered to chlorite, as has part of the groundmass.
AK-81-41	Aphanitic dike. The rock consists of an equigranular mixture of plagioclase and opaque minerals and is partially altered to carbonate.
AK-81-42	Similar to AK-81-41, but vesicular and has a well-developed trachytic texture.

APPENDIX A *(continued)*

Sample	Description
AK-81-43	Hornblende andesite dike. The rock is porphyritic and contains plagioclase, hornblende, and clinopyroxene phenocrysts in a holocrystalline groundmass. The hornblende has reaction rims of plagioclase and opaque minerals.
AK-81-44	Slightly porphyritic andesite dike. The rock contains about 10 percent plagioclase phenocrysts in a fine-grained groundmass of plagioclase and opaques. Both the plagioclase and the groundmass are partially altered to chlorite.
AK-81-45	Similar to AK-81-44, but is slightly coarser grained. The rock also contains xenoliths that have a mineralogy similar to the host rock, but are more highly altered. The amygdules are filled with carbonate.
AK-81-46	Partially altered porphyritic andesite dike. The rock contains plagioclase and clinopyroxene phenocrysts in a trachytic groundmass. The amygdules are filled with carbonate, whereas the groundmass contains both carbonate and chlorite.
AK-81-47	Similar to AK-81-46.
AK-81-48	Similar to AK-81-46, except that carbonate alteration is more pervasive.
AK-81-50	Slightly altered porphyritic basaltic dike. Plagioclase and clinopyroxene phenocrysts in a holocrystalline groundmass. The clinopyroxene exhibits two periods of growth an early state as independent phenocrysts and a late stage where it ophitically encloses groundmass plagioclase laths. The two stages are optically continuous.
AK-81-51	Porphyritic andesite lava flow. The rock contains clinopyroxene, orthopyroxene, plagioclase, and opaque phenocrysts in a trachytic groundmass. Minor amounts of carbonate and chlorite are present.
AK-81-52	Slightly altered porphyritic andesite lava flow. The flow contains plagioclase, orthopyroxene, clinopyroxene, and opaque phenocrysts in a holocrystalline groundmass. The orthopyroxene occurs in trace amounts.
AK-81-53	Altered porphyritic andesite dike. The rock contains plagioclase, clinopyroxene, and altered olivine phenocrysts in a holocrystalline groundmass. The olivine is altered to chlorite. Chlorite-filled amygdules and carbonate-filled amygdules, rimmed by chlorite, are also present.
AK-81-54	Altered andesite dike. A few plagioclase phenocrysts in a very fine grained groundmass. Carbonate and chlorite alteration is pervasive.
AK-81-55	Aphanitic dike. Less than 1 percent plagioclase phenocrysts in a fine-grained trachytic groundmass containing plagioclase and opaque minerals; some chlorite alteration.
AK-81-56	Altered dike. Holocrystalline rock containing less than 1 percent plagioclase phenocrysts in a groundmass composed of plagioclase laths, opaque minerals, and clinopyroxene. Chlorite and carbonate occur as amygdule fillings and in the groundmass.
AK-81-57	Partially altered andesite dike. The dike contains large plagioclase phenocrysts in a very fine grained groundmass. Chlorite alteration is common.
AK-81-57A	Partially altered andesite dike. Similar to AK-81-56.
AK-81-57B	Similar to AK-81-56.

APPENDIX A *(continued)*

Sample	Description
AK-81-58	Similar to AK-81-56.
AK-81-59	Altered andesite dike. The dike contains large plagioclase phenocrysts in a groundmass altering to chlorite.
AK-81-60	Similar to AK-81-59.
AK-81-61	Coarsely porphyritic basaltic dike. The dike contains large plagioclase and minor olivine phenocrysts in a holocrystalline groundmass. There is a great deal of brown alteration material present.
AK-81-62	Partially altered andesite lava flow. The flow contains crystal clots of plagioclase, opaque minerals, and clinopyroxene in a fine-grained trachytic groundmass.
AK-81-63	Andesite lava flow. The flow contains plagioclase phenocrysts in a trachytic groundmass composed of opaque minerals, plagioclase, and clinopyroxene. Olivine was present, but has altered to chlorite. Chlorite and carbonate are present in the groundmass.
AK-81-64	Similar to AK-81-63.
AK-81-65	Porphyritic andesite lava flow. The flow contains olivine, plagioclase, and clinopyroxene phenocrysts in a holocrystalline groundmass. Olivine has oxidized rims but is otherwise unaltered.
AK-81-66	Porphyritic andesite lava flow. The flow contains plagioclase and clinopyroxene phenocrysts in a trachytic groundmass.
AK-81-69	Similar to AK-81-66 but originally contained olivine phenocrysts that have been altered to chlorite.
AK-81-70	Altered andesite dike. The dike contains plagioclase phenocrysts in a groundmass composed of plagioclase, clinopyroxene, and opaque minerals. The groundmass has been partially altered to chlorite and carbonate. Amygdules are filled with chlorite and carbonate.
AK-81-71	Coarsely crystalline andesite dike. The dike contains hornblende, orthopyroxene, and plagioclase phenocrysts. There is very little groundmass present. Carbonate is present as an interstitial filling between grains.
AK-81-72	Porphyritic andesite dike. The dike contains aligned phenocrysts of plagioclase, clinopyroxene, olivine, and opaque minerals in a microcrystalline groundmass.
AK-81-73	Plagioclase, clinopyroxene gabbro. Intrusive rock containing large plagioclase grains ophitically enclosed by clinopyroxene.
AK-81-100	Similar to AK-81-73.
AK-81-101	Porphyritic andesite. Plagioclase and orthopyroxene phenocrysts in a brown glassy groundmass.
AK-81-102	Porphyritic basaltic plug. The intrusion contains clinopyroxene and plagioclase phenocrysts in a groundmass consisting of plagioclase, clinopyroxene, and opaque minerals. The plagioclase phenocrysts commonly contain inclusions of clinopyroxene and opaque minerals.
AK-81-102A	Porphyritic andesite dike. The dike contains plagioclase and phenocrysts in a holocrystalline groundmass.

APPENDIX A *(continued)*

Sample	Description
AK-81-102B	Partially altered andesite dike. The dike contains phenocrysts of olivine, clinopyroxene, and plagioclase in a holocrystalline groundmass.
AK-81-106-1.5-10	Altered andesite dike. The dike contains clinopyroxene and plagioclase phenocrysts in a holocrystalline groundmass. The amount of alteration of the clinopyroxene. . .phenocrysts as well as groundmass. . .increases across the dike. At the top of the dike the mafic minerals are completely altered to chlorite and carbonate.
AK-80-7A	Porphyritic andesite-dacite lava flow. The flow contains plagioclase, orthopyroxene, and clinopyroxene phenocrysts in a very fine grained, unaltered groundmass.
AK-80-8	Similar to AK-80-7A.

APPENDIX B

Microprobe data for Akutan lavas.

[Analyses performed at Alaska Division of Geological and Geophysical Surveys by Roman Motyka. Symbols are as follows: ol - olivine, cpx - clinopyroxene, plag - plagioclase, opx - orthopyroxene, hb - hornblende. Oxide values are in weight-percent]

	Sample AK-81-1										
	Ol core	Ol core	Ol core	Ol rim	Ol rim	Ol rim	Cpx	Cpx core	Cpx core	Cpx core	Cpx rim
Oxides											
SiO_2	38.66	37.95	38.33	38.06	36.77	37.94	52.15	50.98	50.98	52.39	48.90
TiO_2	0.04	0.04	0.09	0.04	0.05	0.03	0.27	0.37	0.41	0.18	0.74
Al_2O_3	0.00	0.02	0.00	0.00	0.00	0.00	2.58	3.32	3.69	1.91	5.90
Cr_2O_3	0.02	0.03	0.05	0.05	0.00	0.01	0.29	0.28	0.13	0.61	0.00
FeO	23.00	27.92	22.83	25.49	30.21	23.69	4.57	5.26	5.45	3.48	8.59
MnO	0.45	0.67	0.49	0.51	0.69	0.47	0.13	0.16	0.14	0.08	0.25
NiO	0.06	0.07	0.05	0.11	0.00	0.10	0.05	0.03	0.03	0.02	0.03
MgO	38.76	35.52	38.93	36.68	31.77	38.05	16.34	16.28	15.74	17.29	14.06
CaO	0.19	0.23	0.19	0.18	0.23	0.20	22.66	22.34	22.86	23.07	20.85
Na_2O	0.02	0.00	0.04	0.00	0.00	0.00	0.29	0.24	0.19	0.17	0.42
K_2O	0.00	0.00	0.00	0.01	0.00	0.01	0.00	0.01	0.01	0.02	0.01
P_2O_5	0.06	0.08	0.06	0.03	0.05	0.06	0.00	0.01	0.02	0.01	0.00
Total	101.26	102.53	101.00	101.16	99.77	100.56	99.33	99.28	99.65	99.23	99.75
	Molecular proportions										
SiO_2	1.028	1.055	1.016	1.024	0.955	1.004	1.895	1.860	1.870	1.897	1.817
TiO_2	0.000	0.001	0.001	0.000	0.001	0.001	0.008	0.010	0.011	0.005	0.021
Al_2O_3	0.000	0.000	0.000	0.000	0.000	0.000	0.111	0.142	0.160	0.082	0.258
Cr_2O_3	0.000	0.001	0.001	0.001	0.000	0.000	0.008	0.008	0.004	0.018	0.000
FeO	0.512	0.649	0.506	0.574	0.683	0.525	0.139	0.160	0.168	0.105	0.267
MnO	0.010	0.016	0.011	0.011	0.016	0.011	0.004	0.005	0.004	0.003	0.008
NiO	0.001	0.001	0.001	0.002	0.000	0.002	0.001	0.000	0.001	0.001	0.001
MgO	1.536	1.472	1.538	1.472	1.281	1.500	0.885	0.885	0.861	0.933	0.779
CaO	0.006	0.007	0.006	0.005	0.008	0.006	0.883	0.873	0.898	0.895	0.830
Na_2O	0.001	0.000	0.002	0.000	0.000	0.000	0.003	0.017	0.013	0.012	0.031
K_2O	0.000	0.000	0.000	0.000	0.000	0.000	0.000	0.000	0.000	0.001	0.000
P_2O_5	0.001	0.002	0.001	0.000	0.001	0.001	0.000	0.000	0.001	0.000	0.000
Total	3.095	3.204	3.083	3.089	2.945	3.050	3.821	3.960	3.991	3.952	4.012
	Sample AK-81-1.*Continued*										
	Cpx rim	Cpx rim	Cpx mid	Cpx mid	Plag core	Plag core	Plag mid	Plag mid1	Plag mid2	Plag rim	Plag rim
Oxides											
SiO_2	50.37	48.56	51.20	48.21	46.19	45.20	46.80	47.21	48.72	46.21	46.40
TiO_2	0.53	0.84	0.42	0.80	0.02	0.03	0.04	0.07	0.03	0.05	0.01
Al_2O_3	4.20	5.47	3.59	5.95	34.34	35.12	33.61	33.47	32.43	34.64	34.42
Cr_2O_3	0.00	0.01	0.25	0.00	0.00	0.03	0.02	0.02	0.01	0.08	0.00
FeO	8.02	9.21	5.37	8.45	0.65	0.67	0.67	0.72	0.73	0.73	0.67
MnO	0.31	0.26	0.16	0.25	0.03	0.00	0.05	0.05	0.00	0.01	0.05
NiO	0.04	0.04	0.04	0.07	0.02	0.04	0.04	0.00	0.01	0.01	0.02
MgO	15.33	13.85	15.59	14.04	0.01	0.06	0.10	0.16	0.10	0.04	0.07
CaO	20.04	20.61	22.74	20.64	17.39	17.68	16.72	16.40	15.25	17.41	17.21
Na_2O	0.27	0.34	0.26	0.35	1.56	1.13	1.87	2.12	2.80	1.65	1.61
K_2O	0.00	0.01	0.01	0.02	0.04	0.05	0.07	0.11	0.10	0.06	0.05
P_2O_5	0.01	0.01	0.01	0.05	0.01	0.02	0.03	0.07	0.01	0.00	0.01
Total	99.12	99.21	99.64	98.83	100.26	100.03	100.02	100.40	100.19	100.89	100.52
	Molecular proportions.*Continued*										
SiO_2	1.845	1.798	1.877	1.770	2.136	2.087	2.155	2.183	2.240	2.155	2.151
TiO_2	0.015	0.023	0.011	0.022	0.000	0.001	0.001	0.003	0.001	0.001	0.000
Al_2O_3	0.181	0.239	0.155	0.257	1.873	1.911	1.825	1.825	1.756	1.903	1.882
Cr_2O_3	0.000	0.000	0.007	0.000	0.000	0.001	0.001	0.001	0.000	0.003	0.000
FeO	0.245	0.285	0.165	0.259	0.025	0.026	0.026	0.027	0.025	0.029	0.026
MnO	0.010	0.008	0.005	0.008	0.001	0.000	0.001	0.001	0.000	0.000	0.003
NiO	0.001	0.001	0.001	0.002	0.000	0.001	0.001	0.000	0.000	0.000	0.000
MgO	0.837	0.764	0.852	0.768	0.000	0.004	0.008	0.012	0.006	0.003	0.004
CaO	0.786	0.818	0.894	0.812	0.862	0.874	0.825	0.813	0.751	0.870	0.855
Na_2O	0.019	0.025	0.018	0.025	0.139	0.102	0.167	0.189	0.249	0.148	0.145
K_2O	0.000	0.001	0.000	0.001	0.003	0.003	0.004	0.007	0.005	0.004	0.003
P_2O_5	0.000	0.000	0.000	0.002	0.000	0.000	0.001	0.003	0.000	0.000	0.000
Total	3.939	3.962	3.985	3.926	5.038	5.010	5.015	5.064	5.033	5.118	5.069

APPENDIX B *(continued)*

Sample AK-81-13

	Ol	Ol core	Ol core	Ol rim	Ol rim	Ol rim	Cpx core	Cpx core
Oxides								
SiO_2	37.87	37.60	38.06	37.69	38.12	37.42	48.88	49.59
TiO_2	0.06	0.01	0.05	0.05	0.02	0.06	0.73	0.69
Al_2O_3	0.05	0.01	0.00	0.00	0.01	0.03	5.17	4.09
Cr_2O_3	0.02	0.02	0.04	0.03	0.01	0.03	0.02	0.02
FeO	23.82	23.20	23.62	24.32	23.58	24.13	7.08	8.61
MnO	0.51	0.47	0.47	0.54	0.46	0.55	0.19	0.30
NiO	0.09	0.03	0.00	0.07	0.08	0.01	0.01	0.05
MgO	38.78	35.15	38.98	38.01	38.95	37.47	14.62	14.72
CaO	0.20	0.19	0.20	0.02	0.18	0.21	21.79	20.58
Na_2O	0.00	0.01	0.00	0.00	0.00	0.02	0.28	0.34
K_2O	0.01	0.00	0.01	0.00	0.00	0.00	0.00	0.01
P_2O_5	0.02	0.05	0.01	0.03	0.00	0.00	0.00	0.03
Total	101.43	96.74	101.44	100.76	101.42	99.93	98.77	99.03
Molecular proportions								
SiO_2	1.016	0.940	1.019	1.007	1.020	0.984	1.785	1.826
TiO_2	0.001	0.000	0.001	0.001	0.000	0.001	0.020	0.019
Al_2O_3	0.001	0.000	0.000	0.000	0.000	0.001	0.223	0.178
Cr_2O_3	0.001	0.001	0.001	0.001	0.000	0.001	0.000	0.001
FeO	0.534	0.485	0.529	0.543	0.528	0.531	0.214	0.266
MnO	0.011	0.010	0.011	0.012	0.011	0.012	0.006	0.009
NiO	0.002	0.001	0.000	0.001	0.001	0.000	0.000	0.001
MgO	1.551	1.310	1.556	1.513	1.554	1.469	0.795	0.807
CaO	0.006	0.005	0.006	0.006	0.005	0.006	0.853	0.811
Na_2O	0.000	0.001	0.000	0.000	0.000	0.001	0.020	0.025
K_2O	0.000	0.000	0.001	0.000	0.000	0.000	0.000	0.001
P_2O_5	0.000	0.001	0.000	0.001	0.000	0.000	0.000	0.000
Total	3.123	2.754	3.124	3.085	3.119	3.006	3.916	3.944

Sample AK-81-13 *Continued*

	Cpx core	Cpx rim	Cpx rim	Plag core	Plag core	Plag rim	Plag rim
Oxides							
SiO_2	48.88	51.30	50.96	45.29	47.40	45.92	50.08
TiO_2	0.78	0.30	0.49	0.00	0.03	0.01	0.06
Al_2O_3	4.80	2.88	2.36	33.46	32.66	33.66	30.78
Cr_2O_3	0.03	0.29	0.00	0.00	0.00	0.01	0.03
FeO	8.18	4.98	8.22	0.64	0.67	0.69	0.85
MnO	0.20	0.17	0.30	0.03	0.01	0.00	0.04
NiO	0.04	0.01	0.01	0.01	0.07	0.00	0.02
MgO	14.50	16.48	15.72	0.06	0.13	0.08	0.14
CaO	21.10	22.24	20.42	17.00	15.72	17.73	13.49
Na_2O	0.36	0.16	0.26	1.59	2.22	1.57	3.54
K_2O	0.00	0.00	0.00	0.05	0.08	0.05	0.14
P_2O_5	0.01	0.04	0.02	0.06	0.06	0.05	0.00
Total	98.88	98.85	98.76	98.19	99.05	99.77	99.17
Molecular proportions *Continued*							
SiO_2	1.796	1.858	1.863	2.045	2.153	2.084	2.266
TiO_2	0.022	0.008	0.014	0.000	0.001	0.000	0.003
Al_2O_3	0.208	0.123	0.102	1.788	1.749	1.801	1.642
Cr_2O_3	0.001	0.008	0.000	0.000	0.000	0.000	0.001
FeO	0.251	0.151	0.251	0.024	0.026	0.026	0.032
MnO	0.006	0.005	0.009	0.001	0.000	0.000	0.001
NiO	0.001	0.000	0.000	0.000	0.003	0.000	0.000
MgO	0.794	0.890	0.856	0.004	0.009	0.005	0.010
CaO	0.831	0.863	0.799	0.822	0.765	0.814	0.654
Na_2O	0.026	0.011	0.019	0.139	0.195	0.138	0.310
K_2O	0.000	0.000	0.000	0.003	0.005	0.003	0.008
P_2O_5	0.000	0.000	0.001	0.001	0.003	0.001	0.003
Total	3.936	3.917	3.914	4.827	4.909	4.872	4.930

APPENDIX B *(continued)*

Sample AK-81-23

	Opx	Opx	Opx core	Opx core	Opx core	Opx rim	Opx rim	Opx rim	Cpx	Cpx
Oxides										
SiO_2	52.82	52.37	52.75	52.60	52.55	52.76	52.53	52.69	50.64	50.38
TiO_2	0.19	0.29	0.24	0.21	0.20	0.24	0.29	0.24	0.50	0.58
Al_2O_3	0.61	1.40	0.95	0.75	0.53	0.79	0.90	0.86	2.18	2.55
Cr_2O_3	0.02	0.02	0.00	0.03	0.04	0.00	0.03	0.00	0.14	0.02
FeO	21.00	20.18	20.24	20.62	21.62	20.39	20.09	20.32	9.96	10.15
MnO	1.05	0.93	1.00	1.14	1.17	1.02	1.03	1.06	0.56	0.56
NiO	0.03	0.00	0.04	0.00	0.04	0.02	0.00	0.00	0.05	0.03
MgO	23.42	23.75	23.67	23.75	22.39	23.68	23.62	23.34	14.86	14.50
CaO	1.55	1.48	1.50	1.52	1.52	1.53	1.52	1.50	19.96	19.90
Na_2O	0.08	0.00	0.00	0.00	0.00	0.04	0.00	0.04	0.39	0.21
K_2O	0.00	0.01	0.00	0.00	0.01	0.02	0.00	0.01	0.00	0.02
P_2O_5	0.02	0.01	0.00	0.00	0.04	0.00	0.01	0.04	0.00	0.00
Total	100.79	100.44	100.39	100.62	100.11	100.49	100.02	100.10	99.24	98.90

Molecular proportions

SiO_2	1.990	1.956	1.969	1.975	1.968	1.975	1.951	1.960	1.878	1.860
TiO_2	0.005	0.008	0.007	0.006	0.006	0.007	0.008	0.007	0.014	0.016
Al_2O_3	0.027	0.061	0.042	0.033	0.023	0.035	0.039	0.038	0.096	0.111
Cr_2O_3	0.001	0.001	0.000	0.001	0.001	0.000	0.001	0.000	0.001	0.001
FeO	0.662	0.630	0.632	0.648	0.677	0.639	0.624	0.632	0.309	0.314
MnO	0.033	0.003	0.031	0.036	0.037	0.032	0.032	0.033	0.018	0.018
NiO	0.001	0.000	0.001	0.000	0.001	0.001	0.000	0.000	0.001	0.000
MgO	1.315	1.322	1.317	1.330	1.250	1.321	1.307	1.294	0.822	0.798
CaO	0.063	0.059	0.060	0.061	0.061	0.061	0.061	0.059	0.794	0.788
Na_2O	0.006	0.000	0.000	0.000	0.000	0.003	0.000	0.003	0.028	0.015
K_2O	0.000	0.001	0.000	0.000	0.001	0.001	0.000	0.000	0.012	0.001
P_2O_5	0.001	0.000	0.000	0.000	0.001	0.000	0.000	0.001	0.000	0.000
Total	4.104	4.041	4.039	4.090	4.026	4.075	4.023	4.027	3.964	3.922

Sample AK-81-23-*Continued*

	Cpx	Cpx	Cpx	Cpx	Plag	Plag	Plag	Plag	Plag mid-1	Plag mid
Oxides										
SiO_2	51.44	51.18	51.33	51.30	54.27	53.82	54.50	54.31	55.46	53.96
TiO_2	0.44	0.46	0.42	0.43	0.06	0.03	0.04	0.01	0.06	0.29
Al_2O_3	1.66	1.81	0.42	1.76	28.23	28.63	28.22	28.26	27.52	27.53
Cr_2O_3	0.00	0.00	0.03	0.02	0.00	0.02	0.03	0.02	0.08	0.03
FeO	9.96	10.72	10.45	9.68	0.53	0.48	0.47	0.49	0.51	1.19
MnO	0.56	0.62	0.60	0.55	0.00	0.04	0.00	0.01	0.05	0.07
NiO	0.03	0.00	0.04	0.00	0.05	0.00	0.00	0.00	0.05	0.05
MgO	15.10	14.80	14.81	15.01	0.02	0.00	0.05	0.05	0.02	0.15
CaO	19.78	19.49	19.80	19.89	10.54	10.65	10.13	10.21	9.51	10.15
Na_2O	0.31	0.38	0.32	0.28	5.43	5.08	5.33	5.27	5.80	5.41
K_2O	0.00	0.01	0.01	0.00	0.23	0.19	0.19	0.22	0.25	0.49
P_2O_5	0.04	0.05	0.05	0.02	0.00	0.00	0.02	0.00	0.03	0.06
Total	99.32	99.52	98.28	98.94	99.38	98.94	98.98	98.83	99.34	99.37

Molecular proportions-*Continued*

SiO_2	1.905	1.908	1.912	1.890	2.437	2.403	2.430	2.419	2.481	2.435
TiO_2	0.012	0.013	0.012	0.012	0.003	0.001	0.001	0.000	0.001	0.009
Al_2O_3	0.073	0.080	0.072	0.076	1.495	1.507	1.483	1.484	1.451	1.465
Cr_2O_3	0.000	0.001	0.000	0.000	0.000	0.001	0.001	0.001	0.003	0.001
FeO	0.309	0.335	0.325	0.299	0.019	0.018	0.018	0.018	0.019	0.045
MnO	0.017	0.020	0.019	0.017	0.000	0.001	0.000	0.000	0.001	0.003
NiO	0.001	0.000	0.001	0.000	0.001	0.000	0.000	0.000	0.001	0.001
MgO	0.834	0.822	0.822	0.824	0.001	0.000	0.004	0.003	0.001	0.010
CaO	0.779	0.790	0.790	0.785	0.492	0.509	0.484	0.487	0.455	0.491
Na_2O	0.219	0.027	0.023	0.020	0.473	0.440	0.462	0.455	0.509	0.473
K_2O	0.001	0.001	0.000	0.014	0.020	0.010	0.010	0.013	0.014	0.029
P_2O_5	0.001	0.002	0.002	0.001	0.000	0.000	0.001	0.000	0.001	0.003
Total	4.151	3.999	3.987	3.938	4.941	4.890	4.894	4.880	4.931	4.965

APPENDIX B *(continued)*

Sample AK-81-23-*Continued*

	Plag rim	Plag rim	Plag rim	Plag core	Plag core	Plag core	Plag core	Plag core	Plag core
Oxides									
SiO_2	53.73	54.74	54.54	56.24	54.53	51.35	54.87	55.69	54.98
TiO_2	0.09	0.05	0.03	0.05	0.05	0.05	0.06	0.08	0.00
Al_2O_3	28.44	27.67	27.69	26.64	28.37	30.40	27.99	27.45	27.57
Cr_2O_3	0.00	0.00	0.01	0.02	0.04	0.04	0.01	0.01	0.05
FeO	0.47	0.53	0.50	0.43	0.48	0.62	0.51	0.46	0.45
MnO	0.01	0.04	0.00	0.01	0.02	0.01	0.04	0.04	0.00
NiO	0.01	0.01	0.01	0.04	0.01	0.00	0.01	0.03	0.02
MgO	0.05	0.01	0.03	0.04	0.03	0.01	0.00	0.05	0.08
CaO	11.05	10.21	10.19	9.04	10.18	12.72	10.02	9.28	9.63
Na_2O	5.29	5.87	5.48	6.25	5.51	4.08	5.41	5.89	5.26
K_2O	0.19	0.33	0.32	0.26	0.20	0.02	0.23	0.26	0.25
P_2O_5	0.03	0.04	0.00	0.00	0.03	0.00	0.00	0.01	0.05
Total	99.36	99.50	98.80	99.02	99.45	99.30	99.15	99.25	98.34

Molecular proportions-*Continued*

SiO_2	2.415	2.463	2.431	2.503	2.447	2.324	2.449	2.485	2.430
TiO_2	0.003	0.001	0.001	0.001	0.001	0.001	0.003	0.003	0.001
Al_2O_3	1.506	1.468	1.455	1.400	1.500	1.621	1.474	1.449	1.437
Cr_2O_3	0.000	0.001	0.000	0.004	0.000	0.000	0.000	0.000	0.001
FeO	0.018	0.020	0.018	0.016	0.018	0.023	0.019	0.017	0.017
MnO	0.000	0.001	0.000	0.000	0.001	0.000	0.001	0.001	0.000
NiO	0.000	0.000	0.000	0.001	0.000	0.000	0.000	0.001	0.000
MgO	0.003	0.000	0.003	0.003	0.003	0.001	0.000	0.004	0.005
CaO	0.532	0.492	0.487	0.431	0.490	0.617	0.480	0.443	0.456
Na_2O	0.461	0.513	0.474	0.540	0.479	0.358	0.469	0.509	0.451
K_2O	0.010	0.012	0.013	0.000	0.014	0.000	0.013	0.014	0.014
P_2O_5	0.001	0.001	0.001	0.000	0.001	0.000	0.000	0.000	0.001
Total	4.949	4.972	4.883	4.899	4.954	4.945	4.908	4.926	4.813

Sample AK-81-71

	Hb core	Hb rim	Opx	Opx	Opx core	Opx rim	Plag core	Plag core	Plag mid	Plag rim
Oxides										
SiO_2	41.86	42.14	52.59	53.04	52.76	51.81	53.64	53.13	53.61	53.51
TiO_2	3.31	3.19	0.29	0.22	0.20	0.27	0.04	0.06	0.04	0.03
Al_2O_3	11.23	11.26	1.30	0.97	0.68	1.29	29.34	29.37	29.32	29.35
Cr_2O_3	0.01	0.00	0.00	0.07	0.03	0.02	0.03	0.05	0.02	0.00
FeO	13.98	14.21	19.37	18.69	20.64	21.99	0.39	0.45	0.46	0.42
MnO	0.44	0.54	1.08	1.05	1.23	1.33	0.00	0.04	0.03	0.02
NiO	0.02	0.05	0.05	0.07	0.08	0.07	0.00	0.02	0.00	0.00
MgO	12.64	12.45	24.16	24.20	22.95	21.23	0.05	0.06	0.04	0.00
CaO	10.47	10.56	1.50	1.51	1.42	1.43	11.30	11.41	11.21	11.11
Na_2O	2.80	3.04	0.00	0.06	0.00	0.05	5.06	4.89	5.13	5.29
K_2O	0.41	0.46	0.00	0.01	0.00	0.00	0.14	0.15	0.13	0.17
P_2O_5	0.02	0.05	0.04	0.04	0.00	0.01	0.00	0.00	0.00	0.00
Total	97.19	97.95	100.38	99.93	99.99	99.50	99.99	99.63	99.99	99.90

Molecular proportions

SiO_2	5.609	5.711	1.955	1.954	1.963	1.930	2.427	2.398	2.428	2.421
TiO_2	0.333	0.324	0.008	0.006	0.006	0.007	0.001	0.003	0.001	0.001
Al_2O_3	1.772	1.801	0.057	0.042	0.030	0.057	1.564	0.562	1.565	1.565
Cr_2O_3	0.000	0.000	0.000	0.002	0.001	0.001	0.001	0.001	0.001	0.000
FeO	1.566	1.613	0.603	0.576	0.641	0.686	0.014	0.017	0.017	0.016
MnO	0.051	0.062	0.034	0.033	0.039	0.042	0.000	0.001	0.001	0.001
NiO	0.004	0.004	0.001	0.002	0.002	0.002	0.000	0.001	0.000	0.000
MgO	2.524	2.515	1.339	1.329	1.273	1.179	0.003	0.004	0.003	0.000
CaO	1.501	1.535	0.059	0.060	0.056	0.057	0.548	0.551	0.544	0.539
Na_2O	0.727	0.798	0.000	0.004	0.000	0.003	0.444	0.428	0.450	0.463
K_2O	0.072	0.080	0.000	0.000	0.000	0.000	0.008	0.009	0.008	0.010
P_2O_5	0.000	0.004	0.001	0.001	0.000	0.000	0.000	0.000	0.000	0.000
Total	14.159	14.445	4.057	4.009	4.011	3.964	5.010	4.975	5.018	5.016

APPENDIX B *(continued)*

[plag - plagioclase, opx - orthopyroxene, cpx - clinopyroxene, ol - olivine. Oxide values are in weight-percent]

	Sample AK-81-73							
	Cpx	Cpx	Cpx core	Cpx core	Cpx rim	Cpx rim	Plag core	Plag core
Oxides								
SiO_2	50.93	50.01	50.68	49.86	51.08	49.21	44.31	45.18
TiO_2	0.72	0.99	0.68	1.15	0.73	0.69	0.04	0.04
Al_2O_3	2.06	3.15	2.07	3.28	1.75	4.39	35.77	35.27
Cr_2O_3	0.03	0.02	0.01	0.00	0.00	0.00	0.00	0.00
FeO	10.16	9.95	10.03	10.50	11.38	11.01	0.49	0.50
MnO	0.33	0.27	0.32	0.30	0.40	0.39	0.03	0.03
NiO	0.00	0.01	0.03	0.04	0.00	0.00	0.01	0.03
MgO	14.54	13.64	14.63	13.83	13.58	12.48	0.02	0.04
CaO	19.90	20.40	20.14	20.02	19.95	18.80	18.78	17.99
Na_2O	0.22	0.25	1.39	0.34	0.25	0.90	0.80	1.24
K_2O	0.00	0.00	0.00	0.02	0.01	0.01	0.03	0.03
P_2O_5	0.02	0.03	0.00	0.03	0.02	0.06	0.00	0.04
Total	98.91	98.72	94.98	99.37	99.15	97.94	100.27	100.39
	Molecular proportions							
SiO_2	1.878	1.841	1.874	1.856	1.900	1.798	2.057	2.096
TiO_2	0.020	0.028	0.019	0.014	0.020	0.090	0.001	0.001
Al_2O_3	0.089	0.137	0.090	0.144	0.077	0.189	1.958	1.929
Cr_2O_3	0.001	0.001	0.000	0.000	0.000	0.000	0.000	0.001
FeO	0.313	0.307	0.310	0.237	0.354	0.336	0.020	0.020
MnO	0.010	0.008	0.010	0.010	0.013	0.012	0.001	0.001
NiO	0.000	0.000	0.001	0.001	0.000	0.000	0.000	0.001
MgO	0.799	0.749	0.806	0.767	0.753	0.680	0.001	0.003
CaO	0.786	0.804	0.798	0.798	0.794	0.736	0.934	0.895
Na_2O	0.016	0.018	0.028	0.025	0.018	0.064	0.072	0.111
K_2O	0.000	0.000	0.000	0.001	0.001	0.000	0.001	0.003
P_2O_5	0.001	0.001	0.000	0.001	0.001	0.002	0.000	0.001
Total	3.912	2.894	3.936	3.944	3.931	3.907	5.045	5.061

	Sample AK-81-73–*Continued*						
	Plag core	Plag mid	Plag mid	Plag rim	Plag rim	Plag rim	Plag rim
Oxides							
SiO_2	45.69	45.50	45.88	51.70	65.17	65.07	56.21
TiO_2	0.04	0.05	0.07	0.05	0.07	0.04	0.06
Al_2O_3	34.63	34.94	34.71	30.53	18.86	18.98	27.14
Cr_2O_3	0.02	0.04	0.02	0.00	0.00	0.01	0.02
FeO	0.52	0.58	0.57	0.71	0.32	0.28	0.46
MnO	0.03	0.00	0.02	0.00	0.03	0.00	0.02
NiO	0.00	0.02	0.01	0.00	0.05	0.02	0.00
MgO	0.02	0.04	0.05	0.09	0.01	0.00	0.04
CaO	17.31	17.59	17.29	12.76	0.22	0.26	9.07
Na_2O	1.48	1.49	1.50	4.25	4.32	4.82	6.19
K_2O	0.04	0.02	0.04	0.19	10.40	9.71	0.37
P_2O_5	0.03	0.05	0.01	0.03	0.01	0.04	0.03
Total	99.87	100.32	100.18	100.31	99.46	99.23	99.61
	Molecular proportions–*Continued*						
SiO_2	2.101	2.108	2.119	2.363	2.941	2.923	2.519
TiO_2	0.001	0.001	0.003	0.001	0.003	0.001	0.003
Al_2O_3	1.877	1.907	1.890	1.645	1.004	1.005	1.433
Cr_2O_3	0.000	0.000	0.000	0.000	0.000	0.000	0.001
FeO	0.020	0.022	0.022	0.027	0.012	0.010	0.017
MnO	0.001	0.000	0.001	0.000	0.001	0.000	0.001
NiO	0.000	0.001	0.000	0.000	0.001	0.001	0.000
MgO	0.001	0.003	0.004	0.007	0.000	0.000	0.003
CaO	0.852	0.873	0.856	0.624	0.010	0.013	0.436
Na_2O	0.131	0.135	0.134	0.376	0.378	0.420	0.538
K_2O	0.003	0.001	0.003	0.012	0.598	0.556	0.021
P_2O_5	0.001	0.001	0.000	0.001	0.000	0.001	0.001
Total	4.989	5.053	5.033	5.056	4.946	4.930	4.973

APPENDIX C

Major oxides analyses and CIPW norms on volcanic rocks from northern Akutan Island

[Analyses performed at Alaska Division of Geological and Geophysical Surveys by M.A. Wiltse and Babette Farris. Abbreviations of normative minerals: ap - apatite, il - ilmenite, mt - magnetite, ab - albite, an - anorthite, qtz - quart, ol - olivine, di - diopside, and hy - hypersthene. Water was not included in the oxide totals or the normative mineral calculations]

Sample	AK-81-1	AK-81-2	AK-81-3	AK-81-5	AK-81-8	AK-81-14	AK-81-23	AK-81-30	AK-81-38	AK-81-39	AK-81-50
Chemical analyses (weight percent)											
Oxides											
SiO_2	49.78	48.99	50.01	51.89	50.63	49.78	56.70	48.89	55.62	55.71	46.04
TiO_2	0.96	0.99	0.97	1.03	0.95	0.96	0.86	1.67	1.10	1.05	1.84
Al_2O_3	17.36	18.78	19.31	18.80	17.41	17.54	17.37	16.90	15.93	16.10	16.95
Fe_2O_3	5.85	3.43	4.70	3.03	3.58	3.95	3.54	2.96	2.96	2.49	4.00
FeO	4.55	6.93	5.45	6.53	6.57	6.21	4.00	10.30	5.36	5.00	6.66
MnO	0.19	0.21	0.20	0.21	0.19	0.19	0.19	0.25	0.20	0.26	0.19
MgO	6.49	5.81	5.06	4.27	6.80	6.19	2.89	5.01	2.53	1.75	7.98
CaO	10.26	10.39	10.11	9.31	10.37	10.20	6.68	10.30	5.72	6.16	11.34
Na_2O	2.74	2.87	2.90	3.40	2.65	2.89	4.16	2.98	4.01	4.49	2.10
K_2O	0.86	0.69	0.80	1.06	0.85	0.98	1.35	0.74	2.17	1.89	0.77
P_2O_5	0.20	0.20	0.22	0.24	0.21	0.22	0.23	0.20	0.33	0.36	0.21
Total	99.24	99.29	100.73	99.77	100.21	99.11	97.97	100.20	95.93	95.26	97.28
CIPW norms (weight percent)											
ap	0.46	0.46	0.51	0.56	0.49	0.51	0.53	0.46	0.76	0.83	0.49
il	1.82	1.88	1.84	1.96	1.80	1.82	1.63	3.17	2.09	1.99	1.90
mt	8.48	4.97	6.81	4.39	5.19	5.73	5.18	4.29	4.29	3.61	5.80
ab	23.19	24.29	24.54	28.77	22.42	24.45	35.20	25.22	33.93	37.99	17.77
or	5.08	4.08	4.73	6.26	5.02	5.20	7.98	4.37	12.82	11.17	4.55
an	32.53	36.32	37.31	32.91	33.10	32.29	24.74	29.71	19.06	18.19	34.55
qtz	2.10	0.00	1.73	1.22	0.27	0.00	9.33	0.00	7.73	7.06	0.00
ol	0.00	4.37	0.00	0.00	0.00	0.00	9.33	6.70	0.00	0.00	9.73
di	13.47	11.33	9.18	9.61	13.72	13.62	5.58	16.69	5.92	8.37	16.35
hy	12.11	11.59	13.08	14.09	18.20	14.44	7.86	9.28	9.33	6.04	6.07
Total	99.24	99.29	99.73	99.77	100.21	99.00	97.98	99.89	95.93	95.25	97.21

Sample	AK-81-51	AK-81-52	AK-81-61	AK-81-62	AK-81-102	AK-80-1A	AK-80-1B	AK-80-1D	AK-80-2A	AK-80-3A
Chemical analyses (weight percent)-*Continued*										
Oxides										
SiO_2	56.43	52.84	49.73	56.70	49.43	53.87	51.56	56.91	56.35	56.97
TiO_2	0.91	0.97	1.07	0.93	0.94	1.40	0.98	0.74	0.83	1.06
Al_2O_3	17.60	18.31	20.06	18.50	17.94	16.61	22.12	18.32	16.90	18.19
Fe_2O_3	3.40	3.63	6.03	3.46	3.24	6.54	4.34	2.83	4.54	2.49
FeO	4.77	5.22	3.51	3.51	5.72	3.60	3.00	5.15	3.87	5.73
MnO	0.17	0.18	0.21	0.16	0.17	0.22	0.14	0.25	0.18	0.21
MgO	3.18	3.82	3.63	2.31	5.85	4.07	2.72	2.78	4.54	2.59
CaO	7.26	8.67	9.65	7.06	11.84	6.17	10.58	7.63	8.67	7.43
Na_2O	3.70	3.74	3.36	4.12	2.92	4.19	3.18	3.91	3.32	4.34
K_2O	1.20	1.00	0.76	1.53	0.87	1.49	0.98	0.85	1.19	0.94
P_2O_5	0.21	0.20	0.33	0.32	0.18	0.42	0.30	0.51	0.23	0.21
Total	98.83	98.58	98.34	98.60	99.10	98.58	100.90	99.88	100.62	100.16
CIPW norms (weight percent)-*Continued*										
ap	0.49	0.46	0.76	0.74	0.42	0.97	0.70	1.18	0.53	0.49
il	1.73	1.84	2.03	1.77	1.79	2.66	1.86	1.41	1.58	2.01
mt	4.93	5.26	8.74	5.02	4.70	8.26	6.29	4.25	6.58	3.61
ab	31.31	31.65	28.43	34.86	23.86	35.45	26.91	33.09	28.09	36.72
or	7.09	5.91	4.49	9.04	5.14	8.80	5.79	5.02	7.03	5.55
an	27.87	30.22	37.41	27.47	33.72	22.11	43.19	29.93	27.70	27.38
qtz	9.90	3.61	3.87	9.32	0.00	6.94	4.76	9.99	9.71	7.46
olv	0.00	0.00	0.00	0.00	3.98	0.00	0.00	0.00	0.00	0.00
di	5.51	9.33	6.47	4.40	18.45	4.48	5.76	3.78	10.86	6.73
hy	10.00	10.30	6.12	5.98	6.75	8.06	4.65	11.33	8.43	10.21
Total	98.83	96.58	100.32	98.60	98.81	97.63	99.90	99.98	100.51	100.16

APPENDIX C *(continued)*

Sample	AK-80-4A	AK-80-5	AK-80-6	AK-80-7A	AK-80-8	AK-80-9B	AK-80-12B	AK-80-14	AK-80-15	AK-80-16
Chemical analyses (weight percent)–*Continued*										
Oxides										
SiO_2	51.78	52.13	57.78	63.18	62.54	49.47	51.87	55.19	55.49	55.21
TiO_2	1.04	0.94	0.88	0.84	0.87	1.15	1.04	1.18	1.16	1.16
Al_2O_3	18.78	17.08	19.00	17.02	16.86	18.47	17.76	17.32	17.40	17.46
Fe_2O_3	5.38	3.37	3.24	3.14	1.42	3.82	4.80	2.98	2.80	3.04
FeO	3.11	5.54	3.65	2.52	2.84	6.15	5.01	6.44	6.57	6.30
MnO	0.13	0.17	0.19	0.20	0.17	0.17	0.23	0.23	0.23	0.23
MgO	4.10	6.16	2.37	1.46	1.37	5.41	4.71	3.74	3.65	3.68
CaO	8.43	10.81	6.79	4.09	4.05	10.84	9.58	7.87	7.98	8.00
Na_2O	2.71	2.57	4.45	5.31	5.38	2.56	3.04	3.83	4.07	4.12
K_2O	0.84	1.16	1.36	1.93	1.90	0.86	0.84	0.85	0.87	0.85
P_2O_5	0.26	0.23	0.25	0.31	0.30	0.23	0.21	0.27	0.21	0.21
Total	96.56	100.06	99.96	100.00	97.10	99.13	99.09	99.90	100.43	100.26
CIPW norms (weight percent)–*Continued*										
ap	0.60	0.53	0.58	0.72	0.70	0.53	0.49	0.63	0.49	0.49
il	1.98	1.79	1.67	1.60	1.65	2.18	1.98	2.24	2.20	2.20
mt	7.43	4.89	4.70	4.55	2.06	5.54	6.96	4.32	4.06	4.41
ab	22.93	21.75	37.65	44.93	45.52	21.66	25.72	32.41	34.44	34.86
or	4.96	6.85	8.04	11.40	11.23	5.08	4.96	5.02	5.14	5.02
an	36.60	31.64	27.85	16.91	16.24	36.37	32.33	27.56	26.64	26.64
qtz	10.12	2.67	8.89	14.67	13.18	1.10	5.20	6.31	5.28	5.03
olv	0.00	0.00	0.00	0.00	0.00	0.00	0.00	0.00	0.00	0.00
di	2.74	16.49	3.40	1.09	1.55	12.87	11.08	8.00	9.55	9.60
hy	8.94	13.56	7.17	4.14	5.57	13.80	10.37	13.22	12.64	12.01
Total	96.30	100.17	99.96	100.01	97.70	99.13	99.09	99.91	100.44	100.26

APPENDIX D
Application of discriminant functions

The following discriminant functions were produced by the stepwise multiple discriminant analysis (Jennrich and Sampson, 1981) and are listed in the text. P_2O_5 and TiO_2 are in weight-percent.

WestF $X = 100.33TiO_2 + 264.09P_2O_5 - 83.22$
EastF $X = 93.55TiO_2 + 245.03P_2O_5 - 72.26$
WestD $X = 151.90TiO_2 + 414.89P_2O_5 - 194.84$
EastD $X = 125.68TiO_2 + 343.05P_2O_5 - 133.74$

A particular case is classified into the group where the value of the discriminant function is the largest. For example, AK-81-61, a dike from Hot Springs Bay, containing 0.33 percent P_2O_5 and 1.07 percent TiO_2. Putting these values into the four discriminant functions produces the values listed below:

WestF $107.35 + 87.15 - 83.22 = 111.28$
EastF $100.10 + 80.86 - 72.26 = 108.69$
WestD $162.53 + 136.91 - 194.84 = 104.60$
EastD $134.48 + 113.21 - 133.74 = 113.95$

The value for EastD is the largest and AK-81-61 would be classified with that group.

APPENDIX E

Rb and Sr analyses

[Samples AK-81-8A, -8B and AK-52A, -52B were duplicates submitted to test the reproducibility of the analyses. ND - no determination]

Sample	Rb (ppm)	Sr (ppm)	Rb-Sr
AK-81-1	21	442	0.050
AK-81-2	ND	455	ND
AK-81-3	16	465	0.034
AK-81-5	10	480	0.021
AK-81-8A	22	440	0.050
AK-81-8B	13	440	0.029
AK-81-11	11	430	0.025
AK-81-14	19	430	0.044
AK-81-17	29	310	0.094
AK-81-22	71	205	0.346
AK-81-23	31	305	0.102
AK-81-24	33	335	0.098
AK-81-26	27	365	0.074
AK-81-30	12	405	0.030
AK-81-31	12	460	0.026
AK-81-33	49	325	0.151
AK-81-51	31	355	0.087
AK-81-52A	31	290	0.107
AK-81-52B	25	290	0.086
AK-81-102	20	350	0.057
AK-80-9A	25	355	0.070
AK-80-11	26	330	0.079